EFFECTS OF FUEL PROPERTIES AND ATOMIZATION ON IGNITION IN A T63 GAS TURBINE COMBUSTOR

INTERIM REPORT
BFLRF No. 235

By

D.W. Naegeli
L.G. Dodge
Belvoir Fuels and Lubricants Research Facility (SwRI)
Southwest Research Institute
San Antonio, Texas

Prepared for

Naval Air Propulsion Center
Trenton, NJ

Under Contract to

U.S. Army Belvoir Research, Development
and Engineering Center
Materials, Fuels and Lubricants Laboratory
Fort Belvoir, Virginia

Contract No. DAAK70-87-C-0043

December 1987

DTIC
ELECTE
MAR 2 2 1989
H

Disclaimers

The findings in this report are not to be construed as an official Department of the Navy or Department of the Army position unless so designated by other authorized documents.

Trade names cited in this report do not constitute an official endorsement or approval of the use of such commercial hardware or software.

DTIC Availability Notice

Qualified requestors may obtain copies of this report from the Defense Technical Information Center, Cameron Station, Alexandria, Virginia 22314.

Disposition Instructions

Destroy this report when no longer needed. Do not return it to the originator.

SECURITY CLASSIFICATION OF THIS PAGE

REPORT DOCUMENTATION PAGE

1a. REPORT SECURITY CLASSIFICATION UNCLASSIFIED		1b. RESTRICTIVE MARKINGS None			
2a. SECURITY CLASSIFICATION AUTHORITY N/A		3. DISTRIBUTION/AVAILABILITY OF REPORT Approved for public release: distribution unlimited			
2b. DECLASSIFICATION/DOWNGRADING SCHEDULE N/A					
4. PERFORMING ORGANIZATION REPORT NUMBER(S) Interim Report BFLRF No. 235		5. MONITORING ORGANIZATION REPORT NUMBER(S)			
6a. NAME OF PERFORMING ORGANIZATION Belvoir Fuels and Lubricants Research Facility (SwRI)	6b. OFFICE SYMBOL (If applicable) N/A	7a. NAME OF MONITORING ORGANIZATION U.S. Army Belvoir Research, Development and Engineering Center			
6c. ADDRESS (City, State, and ZIP Code) Southwest Research Institute 6220 Culebra Road San Antonio, TX 78284		7b. ADDRESS (City, State, and ZIP Code) Fort Belvoir, VA 22042			
8a. NAME OF FUNDING/SPONSORING ORGANIZATION Naval Air Propulsion Center	8b. OFFICE SYMBOL (If applicable) PE33	9. PROCUREMENT INSTRUMENT IDENTIFICATION NUMBER DAAK70-85-C-0007, WD33 ; DAAK70-87-C-0043			
8c. ADDRESS (City, State, and ZIP Code) Trenton, NJ 08628		10. SOURCE OF FUNDING NUMBERS			
		PROGRAM ELEMENT NO.	PROJECT NO.	TASK NO.	WORK UNIT ACCESSION NO.

11. TITLE (Include Security Classification)

Effects of Fuel Properties and Atomization on Ignition in a T63 Gas Turbine Combustor (U)

12. PERSONAL AUTHOR(S)

Naegeli, David W. and Dodge, Lee G.

13a. TYPE OF REPORT Interim	13b. TIME COVERED FROM 6/85 TO 12/87	14. DATE OF REPORT (Year, Month, Day) 1987 December	15. PAGE COUNT 71

16. SUPPLEMENTARY NOTATION

17.	COSATI CODES		18. SUBJECT TERMS (Continue on reverse if necessary and identify by block number)
FIELD	GROUP	SUB-GROUP	Atomization Ignition
			Fuel Effects Fuel Sprays
			Alternative Fuels T63

19. ABSTRACT (Continue on reverse if necessary and identify by block number)

Experiments were performed in a T63 gas-turbine combustor to gain a better understanding of the roles played by fuel properties, atomization, and air velocity and temperature in cold-start ignition. These results were used to improve the characteristic time model for ignition in gas-turbine combustors. Ignition tests were performed on ten fuels while varying reference velocity, burner inlet temperature, fuel/air ratio, and the Sauter Mean Diameter of the fuel spray. Fuel viscosity and volatility were varied over a wide range. The test fuels ranged from gasoline to a heavy marine gas oil (HMGO). Two fuel groups were blended with identical viscosities, but with strikingly different 10 percent boil-off temperatures. To examine the effect of fuel composition on ignition, two fuels were blended with unusually high aromatic contents. Droplet size and spray structure were varied by using six atomizers with different

(CONT'D)

20. DISTRIBUTION/AVAILABILITY OF ABSTRACT ☐ UNCLASSIFIED/UNLIMITED ☒ SAME AS RPT. ☐ DTIC USERS	21. ABSTRACT SECURITY CLASSIFICATION UNCLASSIFIED	
22a. NAME OF RESPONSIBLE INDIVIDUAL Mr. F.W. Schaekel	22b. TELEPHONE (Include Area Code) (704) 664-3576	22c. OFFICE SYMBOL STRBE-VF

DD FORM 1473, 84 MAR   83 APR edition may be used until exhausted.   SECURITY CLASSIFICATION OF THIS PAGE

All other editions are obsolete.

19. Abstract (Cont'd)

flow capacities. Atomizers included the standard T63 dual-orifice, pressure-swirl atomizer and five Delavan simplex pressure-swirl atomizers that varied in flow number.

Average drop sizes, represented by the Sauter Mean Diameter (SMD) were measured for the six atomizers spraying five test fluids using a Malvern laser-diffraction drop-sizing instrument. The SMD's were correlated with fuel properties and atomizer flow parameters.

The airflow velocity at the spark gap was measured by a hot-film anemometer probe. Fuel/air ratios were measured at the spark gap using a heated sampling probe, a catalytic oxidizer, and instrumentation to analyze for CO, CO_2, O_2, and total hydrocarbons.

High-speed photographs of the ignition process were obtained with a Hy-Cam camera and a periscope device mounted on the turbine inlet section of the combustor.

The fuel/air ratios necessary to achieve ignition at various flow conditions were correlated with combustor flow conditions, atomizer parameters, fuel properties, and SMD. The ignition data were then used to improve and verify the characteristic time model.

Significant results included the following:

1. Viscosity, which determined atomization characteristics, was more important than volatility in the ignition process.

2. Ignition depended more strongly on achieving a critical average drop size (SMD) than on reaching the lean-limit fuel/air ratio.

3. Fuel temperature appeared to be more important than air temperature for low-temperature ignition. The fuel temperature was important for its effect on viscosity. A practical implication is that fuel heating, which requires much less heat input than inlet air heating, would be effective in improving cold-start performance.

4. High-speed photography showed significant delays (up to 12 ms) from the time the spark formed the ignition kernel to the onset of visible flame radiation. This observation, combined with results for fuel chemistry effects, indicated that many of the critical steps for ignition occur at temperatures much lower than adiabatic stoichiometric flame temperatures.

5. Two assumptions used in the characteristic time model regarding conditions at the spark gap were verified.

EXECUTIVE SUMMARY

Problems and Objectives: The fuel quality/availability ratio has become complex in recent years because of the uncertainty in the supply of petroleum. The trend toward reduced volatility and increased viscosity could result in the degradation of cold-start ignition, altitude relight, and flame stabilization in gas turbine engines. Difficulty in developing a universal predictive model to correlate ignition data from practical combustors stems from the fact that the physics of the ignition process is not well understood. The purposes of the present study were to (1) provide a clearer definition of which fuel property, viscosity or volatility, plays the more important role in the ignition process, (2) give experimental verification of assumptions used in previous ignition model correlations, and (3) create a data base for effectively verifying ignition models.

Importance of Project: In the design of future gas turbine combustors, it is important to develop useful models for predicting combustion performance. Improved combustion models usually emerge from a more basic understanding of combustion processes. Since the ignition process in gas turbine engines is not well understood, it is important that fundamental studies be performed.

Technical Approach: Experiments were performed to determine the effects of fuel properties, atomization and flow conditions on ignition in a T63 gas turbine combustor. Fuels ranging from JP-4 to naval distillate fuel (NDF) were blended to discern differences in the effects of volatility and viscosity on ignition. Six atomizers were used in the combustor to investigate the effect of droplet size in the fuel spray on ignition. Several experiments were performed to characterize the conditions at the spark gap and observe the ignition kernel. Relatively fundamental measurements of gas velocity and fuel/air ratio were made at the spark gap. High-speed photographs were obtained of the ignition process showing the creation of the ignition kernel, the dark induction period, and the onset of flame propagation. Droplet-size measurements were made with a laser diffraction light scattering technique, and the measured Sauter mean diameters were correlated with fuel properties and atomizer flow conditions. Finally, characteristic time calculations were used in correlating the data, and the validity of that model was examined.

Accomplishments: Several important findings concerning the validity of the characteristic time model for ignition were derived from the experimental investigation. The results confirmed two of the assumptions in the characteristic time model concerning gas velocity and fuel/air ratio at the spark gap. However, the overall conclusion of the work was that significant revisions in the philosophy of the model are required with regard to chemical heat generation and heat loss mechanisms in the ignition kernel.

Military Impact: To be prepared in crisis situations in which the fuel quality/availability ratio is severely compromised, it will be necessary to produce emergency fuels from blends of whatever is available. If the military is to cope with this situation, which may continue to worsen because of increased variability in fuel sources, it is important that the effects of fuel properties such as viscosity and volatility on ignition and flame startability in gas turbine engines are well understood. This understanding is important to the military because it enhances emergency fuel strategies, and provides basic information for the development of advanced gas turbine engines.

FOREWORD/ACKNOWLEDGEMENTS

TABLE OF CONTENTS

LIST OF ILLUSTRATIONS

LIST OF ILLUSTRATIONS (Cont'd)

LIST OF ILLUSTRATIONS (Cont'd)

LIST OF TABLES

I. INTRODUCTION

The fuel quality/availability ratio has become complex in recent years because of the uncertainty in the supply of petroleum. Alternatives, such as synfuels, tend to have different boiling point distributions and increased viscosities when compared with their petroleum equivalents. This trend toward reduced volatility and increased viscosity will result in the degradation of cold start ignition, altitude relight, and flame stabilization in gas turbine engines.

Combustor rig tests have been effectively used to demonstrate the effects of varying fuel properties on ignition and flame stabilization.(1-11)* Analytical models have been developed, such as the characteristic time model, that show promise in correlating ignition (12-15) and flame stabilization (16) data from several combustors.

Recent efforts (17, 18) to correlate ignition data from several practical combustors using the characteristic time model have shown some promise, but a better understanding of the physics of the ignition process is needed before the differences in the correlations for the various engines can be reconciled, and a universal predictive model can be formulated. The recent efforts indicated that the fundamental assumptions in the model needed to be tested through experiments in a practical combustor.

It has been found (18) that the model is quite sensitive to the drop-size distribution in the fuel spray, characterized by the Sauter Mean Diameter (SMD), but this sensitivity has not been properly measured in any of the combustor data available to date. Previous studies (13-15) have employed correlations that were based on measurements of SMD in sprays from atomizers that were similar, but not sensitive to the subtle differences in the design of the actual fuel atomizers used in gas turbine combustors. Also, conditions at the spark gap, i.e., the ignition energy, gas velocity, and the fuel/air ratio, are essential to the model. The gas velocity near the spark gap has always been assumed to be proportional to the reference velocity through the combustor. In previous attempts to correlate ignition data using the characteristic time model, reasonable correlations were found only when the equivalence ratio at the spark gap was assumed to be constant.(17, 18) These

---

* Underscored numbers in parentheses refer to the references at the end of this report.

assumptions about spark gap conditions have not previously been verified with experimental measurements.

To verify the model, basic measurements were required at the spark gap, and combustor data were needed over a wide range of fuel properties, burner inlet temperatures, and atomization conditions.

The purposes of the present study were to (1) provide a clearer definition of which fuel property, viscosity or volatility, plays the more important role in the ignition process, (2) give experimental verification of assumptions used in previous characteristic time model correlations, and (3) create a data base for effectively verifying the characteristic time model.

II. BACKGROUND

A. General

Several aspects of ignition in gas turbine engines are not clearly understood. Although the effects of combustor inlet air temperature, fuel temperature, airflow rate, and reference velocity have been examined in previous ignition studies, little emphasis has been placed on distinguishing the effect of fuel viscosity and volatility, which are related to fuel atomization and evaporation. Atomization is a crucial factor that can be measured accurately by a laser diffraction light scattering technique.(19)   Several studies have been carried out in which Sauter Mean Diameters (SMD) of droplets in sprays have been measured and successfully correlated with atomizer fuel flow conditions and fuel properties.   The fuel properties used in these correlations are fuel density, surface tension, and viscosity.

Fuel density is significant in the correlations only because it affects the mass flow rate and pressure drop through the atomizer. Surface tension is known to play an important role in the mechanism of atomization, but its variation among jet fuels is slight so its effect on the relative drop size is small. Contrarily, while viscosity is less strongly tied to the atomization mechanism, it varies greatly with the fuel type and the fuel temperature. As a result, most studies have shown that viscosity is the most important fuel property in correlating fuel effects on atomization.

The other parameters of importance in modeling ignition are the conditions at the spark gap, i.e., the spark energy, the gas velocity, and fuel/air ratio. Ignition energies can be measured and are usually available from the engine manufacturer. In earlier approaches to modeling, gas velocities at the spark gap were assumed to be proportional to the reference velocity through the combustor. The fuel/air ratio is much more difficult to ascertain; the fuel is present in both liquid and vapor forms, and the distribution of fuel droplets within the combustor is not homogeneous, but instead, depends strongly on the airflow patterns. These conditions must be well-known if a predictive ignition model is to be developed and verified.

B. Characteristic Time Ignition Model

The characteristic time model (CTM) is based on the assumption that the spark energy heats a fuel/air mixture homogeneously within a kernel of finite dimensions. The criterion for ignition is that the heat generated within the kernel volume is greater than the heat lost. In a typical gas turbine combustor employing a recirculation-stabilized spray diffusion flame, the physicochemical processes responsible for ignition may be expressed in terms of three rate processes. Since fuel must evaporate to burn, heat generation is limited first by droplet evaporation and then by the rate of chemical reaction. The heat loss from the spark kernel is controlled by turbulent mixing and conduction losses to the spark plug. Assuming that the conduction losses are negligible because the spark kernel is rapidly swept away from the spark plug, it is apparent that an ignition limit is reached when the rate of turbulent mixing (heat loss) is balanced by the sum of the rates of chemical reaction and fuel evaporation (heat generation). The CTM approach to analyzing the ignition process is that of expressing heat generation and loss rates in terms of times, T_{sl}, the turbulent mixing time, T_{hc}, the chemical reaction time, and T_{eb}, the droplet evaporation time.([12], [15]) The ignition limit may then be expressed as

$$T_{sl} \sim T_{hc} + aT_{eb} \qquad (1)$$

where the constant weighing factor, a, is required because these times are only representative of the actual physicochemical processes and are not expected to be quantitatively exact unless basic measurements of gas velocity and temperature, droplet size, ignition energy, and chemical reaction rates are known at the spark gap.

The turbulent mixing time is approximated as a length scale divided by a velocity within the combustor

$$T_{sl} = d_q/V_{ref} \qquad (2)$$

The spark kernel consists of a small volume of fuel and air that is assumed to be heated to the stoichiometric adiabatic flame temperature by the minimum ignition energy, E_{min}, produced by the spark. The spark kernel diameter, d_q, is then

calculated from

$$d_q = \left[\frac{6E_{min}}{\pi \rho_a\, C_{pa}\, (T_{fl} - T_f)} \right]^{1/3} \qquad (3)$$

where C_{pa} is the heat capacity of air at 1300K, T_{fl} is the stoichiometric flame temperature, and T_f is the fuel temperature. Note in Eq. (1) that the reference velocity through the combustor is used because it is proportional to the gas velocity at the spark gap. The reference velocity is calculated from airflow and the maximum cross-sectional area of the combustor.

The droplet evaporation time is calculated from the "d^2" law of Godsave (20)

$$T_{eb} = d^2/\beta \qquad (4)$$

where d is usually taken as the Sauter Mean Diameter, SMD, of the fuel spray, and the evaporation coefficient, β, is calculated from

$$\beta = (8k_a/C_{pa}\, \rho_f)\, \log\,(1 + B)\,(1 + 0.3Re^{0.5}Pr^{0.3}) \qquad (5)$$

where the transfer number B is expressed as

$$B = \frac{C_{pa}\,(T_{fl} - T_{10})}{\Delta H_{vap}} \qquad (6)$$

and the last term, $(1 + 0.3Re^{0.5}Pr^{0.3})$, is the Ranz-Marshall expression (21) to account for enhancement of evaporation by forced convection.

The chemical time is based on an Arrhenius expression for the ignition of homogeneous gas phase lean fuel/air mixtures. It may be expressed as

$$T_{hc} = \frac{b \exp\,(E/RT_{\phi=1})}{\rho_b} \qquad (7)$$

where b is a reciprocal preexponential factor (10^{-5} ms-g-cm^{-3}), and E is an activation energy. Fenn (22) suggests an activation energy of 26,100 cal/mole,

which is representative of a wide range of hydrocarbons and equivalence ratios ranging from about 0.7 to 1.0. At adiabatic stoichiometric flame temperatures usually used in CTM calculations, the chemical reaction time calculated from Eq. (7) is negligible compared with the drop evaporation time calculated from Eq. (4). However, the results presented in this report suggest that much lower temperatures, e.g., the autoignition temperatures of the fuels, are important to the ignition process. At these temperatures, the chemical reaction time is still shorter than the drop evaporation time, but it is not negligibly short.

III. APPROACH: Experimental Facilities and Methods

A. General Description

This work was performed in the combustor facility of the Belvoir Fuels and Lubricants Research Facility (BFLRF) at Southwest Research Institute (SwRI). The combustor facility was specially designed to study fuel-related problems in the operation of gas turbine engines. The air supply system provides a clean, smooth flow of air to the combustion test cell with mass flow rates up to 1.1 kg/s, pressure to 1620 kPa (16 atm), and temperatures from 239K (-30°F) to 1086K (1500°F) (unvitiated). Turbine flowmeters and strain-gage pressure transducers are used to measure flow properties of the air and fuel. Thermocouples are referenced to a 338.5K (150.0°F) oven. Data reduction may be performed on-line with test summaries available immediately; these summaries provide average flow data as well as standard deviations (typically less than 1 percent of average value) of inlet temperature and pressure, exhaust temperature, flow rates of fuel and air, emissions data, and combustion efficiencies.

B. T63 Combustor Rig

The combustor used in this study was fabricated from T63 engine hardware. This combustor has been used in previous programs to study the fuel effects on ignition, combustion stability, combustion efficiency, exhaust pattern factor, radiation, and smoke. Fig. 1 is a schematic of the combustor can showing the location of the fuel atomizer, igniter, and the radiation sensor used to detect the onset of a visible flame in the ignition measurements.

The T63 combustor employs a dual-orifice pressure-swirl atomizer. The primary orifice has a relatively low flow number (7.14×10^{-6} kg/s - $\sqrt{Pa}$) and is used principally for the atomization of fuel in the ignition process. The secondary orifice does not contribute until the fuel flow rate is above that used for ignition.

To further examine the effects of atomization on ignition, an adapter was constructed to allow use of single-orifice, Delavan pressure-swirl atomizers with flow capacities ranging from approximately 4 to 8 gal./hr at a differential fuel
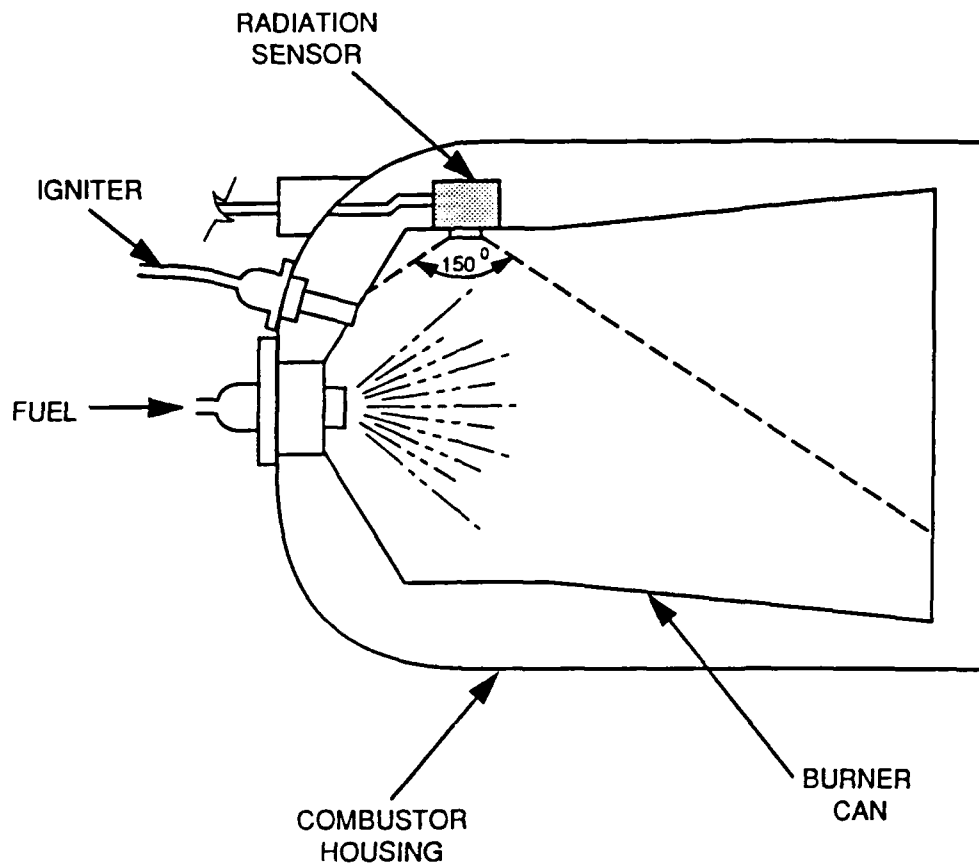
Figure 1. Schematic of T63 combustor

pressure of 100 psi. The combustor was equipped with an igniter that produces sparks at a rate of 8 per second, with energies of approximately 0.87 joules.

C. Combustor Facility

A detailed layout of the BFLRF combustor laboratory is shown in Fig. 2. The facility consists of a variable pressure-temperature air supply, a control room for operating the airflow system, the fuel flow system, the combustor and its exhaust system; also, there are components for the data acquisition system (see Figs. 3 and 4 for views of the control panel).

1. Airflow System

A flow diagram of the "air factory" is shown in Fig. 5. The compressed air for the lab is generated in two stages: two rotary-screw compressors are connected in parallel, each delivering 0.573 m^3/sec (1000 SCFM) at 700 kPa (100 psig). This air
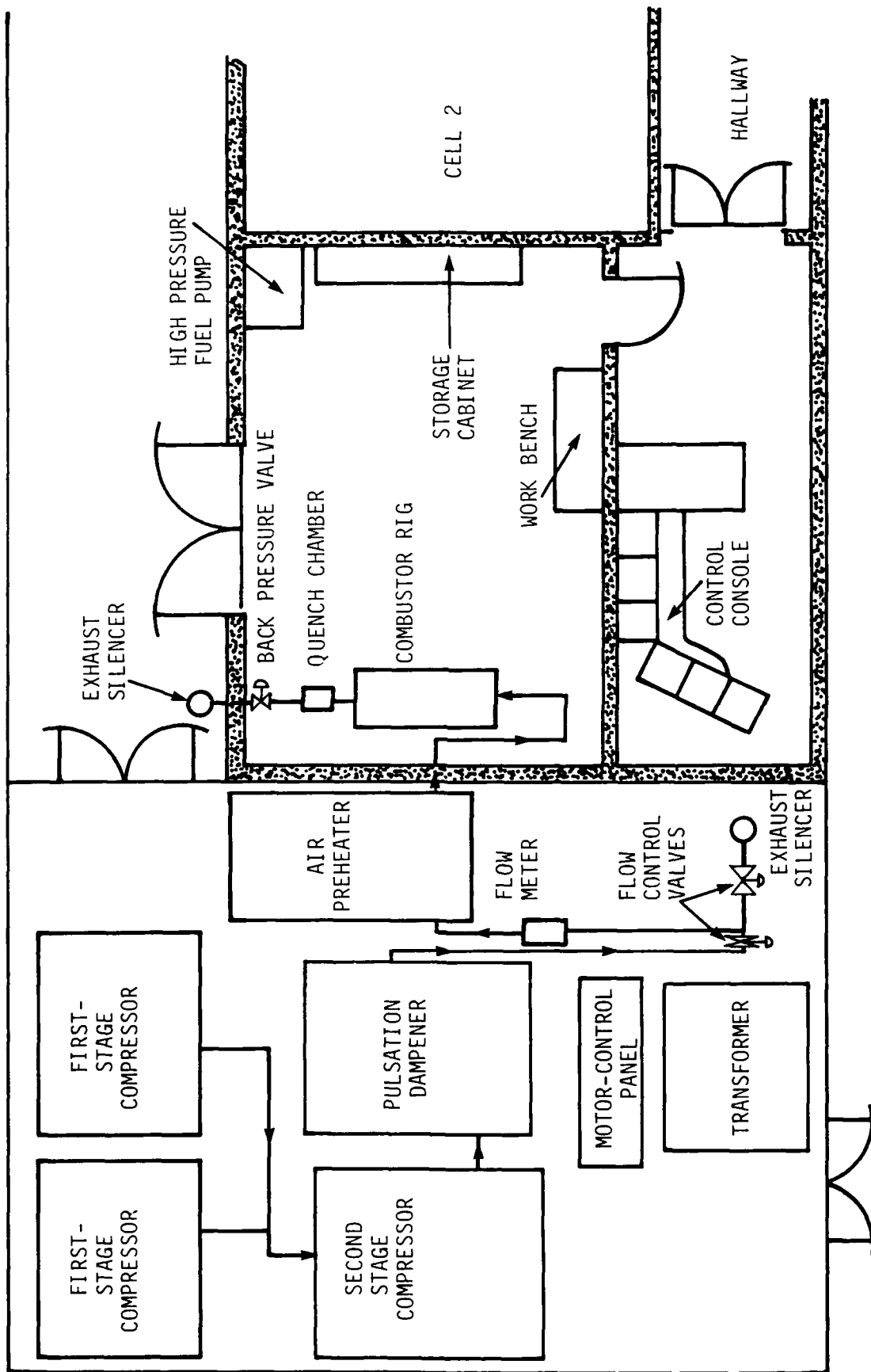
Figure 2. Layout of turbine fuel research combustor laboratory

9
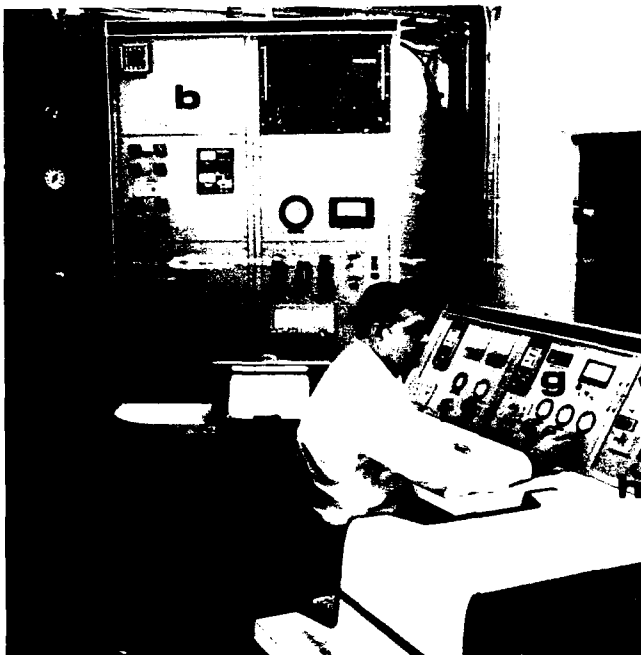
a. Air Heater Control System
b. Compressor Motor Controls
c. Pressure Transducer Reference System
d. Thermocouple Reference Oven
e. Moisture Readout
f. Quench Water Control
g. Air Flow Control
h. Ignition and Fuel Flow Control
i. Window Looks Into Combustion Room

Figure 3. View of control console

a. Programmable Calculator
b. Printer
c. X-Y Plotter
d. Scanner and Digital Voltmeter
e. Magnetic Tape Cassette

Figure 4. View of control console showing data acquisition system

PRESSURE CONTROL

EXHAUST
EXCESS
FLOW

TEMPERATURE
CONTROL

COMPRESSOR

PULSATION
DAMPENER

FLOW
CONTROL

FUEL

WATER

BACK
PRESSURE
VALVE

OIL
FILTER

PRESSURE
CONTROL
VALVE

FLOW
CONTROL
VALVE

TURBINE
FLOW
METER

AIR
PREHEATER

COMBUSTOR
RIG

QUENCH
CHAMBER

EXHAUST
SILENCER
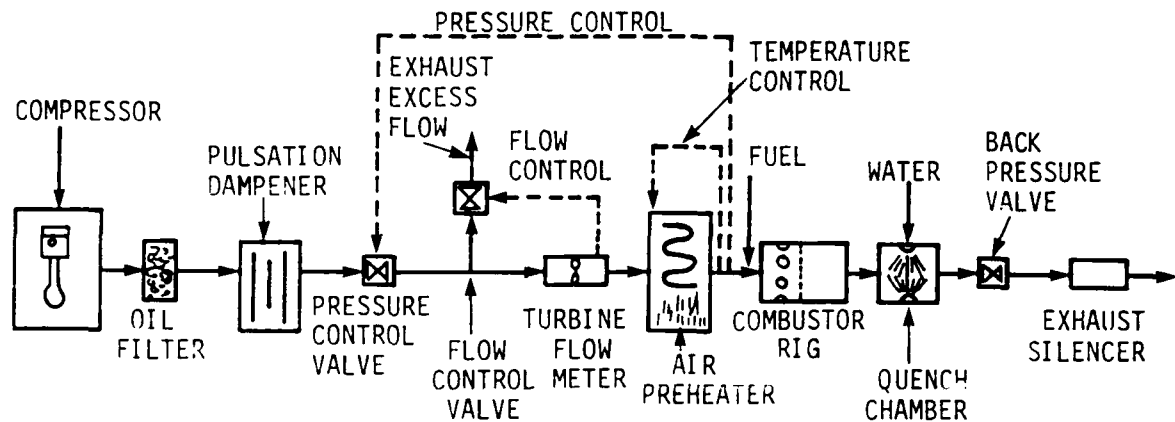
Figure 5. **Flow diagram of turbine combustor system**

goes through an inter-cooler and then to a single-cylinder reciprocating compressor, which compresses it to 1.75 MPa (250 psia). From there, the air passes through an aftercooler, a receiver, and an oil filter before going to the flow controls.

The oil carry over is less than 5 ppm. Suction and discharge bottles are on the booster compressor, which, in conjunction with the receiver, were designed on an analog computer to eliminate pulsations from the airflow. At the downstream side of the receiver, the pressure fluctuation (a frequency of about 45 Hz) was less than 700 Pa (0.1 psi) when the actual pressure was 1.6 MPa (235 psia).

The flow control system operates in two parts: one valve is used to provide a pressure drop to the system, while a second valve bypasses any excess airflow through an exhaust silencer. The compressors are always operating at full capacity--a method that uses more total energy but eliminates any surging caused by the compressors cycling.

A 3-inch (7.62-cm) turbine flowmeter is used to measure the airflow rates. Because a turbine meter measures volumetric flow, the pressure and temperature are also sensed at the meter so the flow measurement can be converted to mass flow rate. The airflow then enters a preheater that is able to heat the flow from roughly 310K (100°F) to 1116K (1550°F). This heater is an indirect, gas-fired system with a counterflow heat exchanger; the air remains unvitiated. The combustion control system was designed in accordance with federal safety standards. The preheater

will shut down automatically in event of a malfunction in the fuel supply or when temperatures exceed established limits. The final air temperature is automatically controlled by a Honeywell recorder-controller system that regulates the air/fuel ratio in the combustion chamber and dilutes the hot exhaust gases going to the tube bundle.

The airflow is piped into the test cell and, for all practical purposes, is the same as the air from any turbine engine compressor. It is essentially pulsation and oil free, and its moisture content is controlled. The airflow rate, pressure, and temperature are independently adjustable to any value within the operating envelope.

2. Cold Air Supply

In order to perform cold start ignition tests, a capability to cool the combustor inlet air supply had to be incorporated into the air supply system. Combustor inlet air was cooled by injecting liquid nitrogen and gaseous oxygen through a manifold placed upstream of the combustor. A rotometer was used to measure the oxygen flow rate, and the oxygen concentration was measured at the combustor exhaust by an oxygen analyzer. Note that fuel was not injected during this measurement. To set a particular flow condition, the oxygen flow was increased until the oxygen concentration was the same as that of air (approximately 21 percent). The net mass flow rate of combustor inlet air was then determined by adding the compressor air flow, measured by the turbine flow meter, the oxygen flow, measured by the rotometer, and the liquid nitrogen flow, calculated in terms of the oxygen flow.

The liquid nitrogen cooling system is capable of lowering the temperature of the burner inlet air supply to -30°F (-34°C) for the mass flow rates (0.2 to 0.6 lb/s) used in the T63 combustor ignition tests.

3. Fuel Supply System

The fuel supply system is capable of pumping fluids ranging in properties from gasoline to No. 5 diesel at flow rates of over 0.063 lb/s (1 gal./min) and pressures up to 7 MPa (1000 psi). For this program, the fuel was forced from drums to the fuel selection manifold system (see Fig. 6) with pressurized inert gas. The manifold
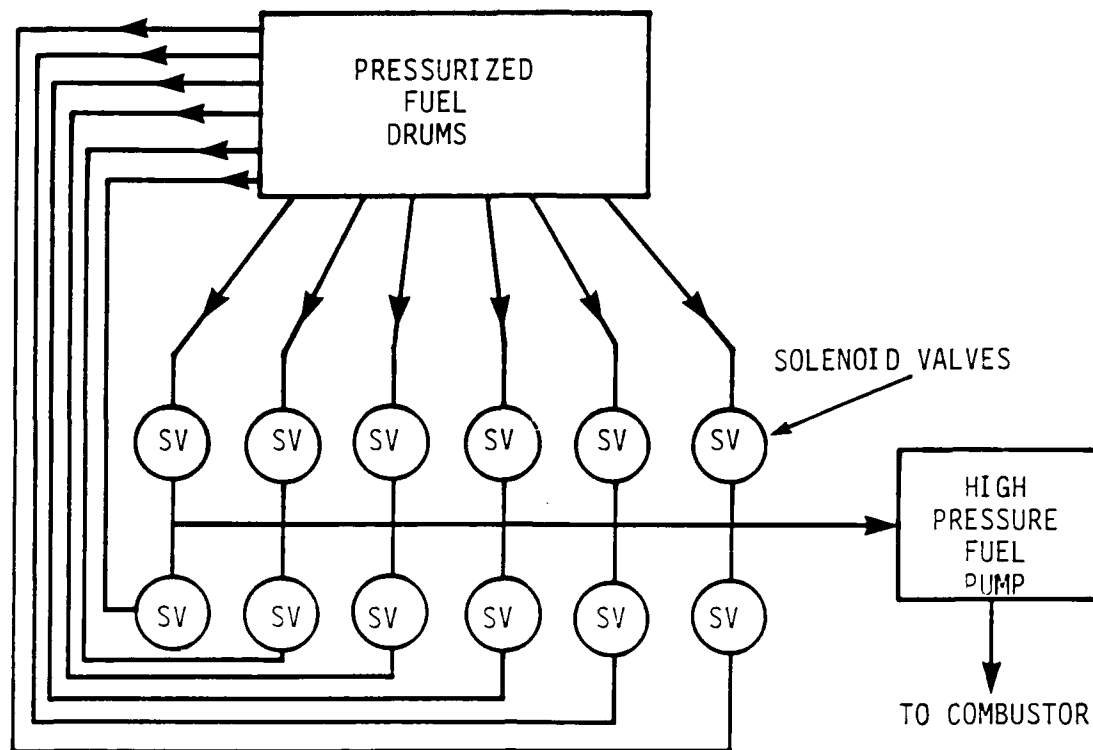
Figure 6. Fuel selection manifolding system

employs 12 solenoid valves (for 12 fuels). After the manifold, a high-pressure pump delivers fuel to the combustor. The plumbing from the pump to the combustor is stainless steel to facilitate cleaning when special fuel blends that threaten to contaminate the system are used. A turbine flowmeter measures the flow rate of the fuel. On shutdown, the lines can be drained and purged with an inert gas.

4. Exhaust System

A pneumatically-controlled valve is located downstream of the quench section to maintain the pressure in the combustor system. A silencer is used to attenuate the exhaust noise.

D. Data Acquisition System

The data acquisition system used a programmable calculator with associated hardware. Fig. 7 shows a flowchart of the system. A digital voltmeter is coupled to a 50-channel scanner that samples the voltage outputs from the various sensor

13
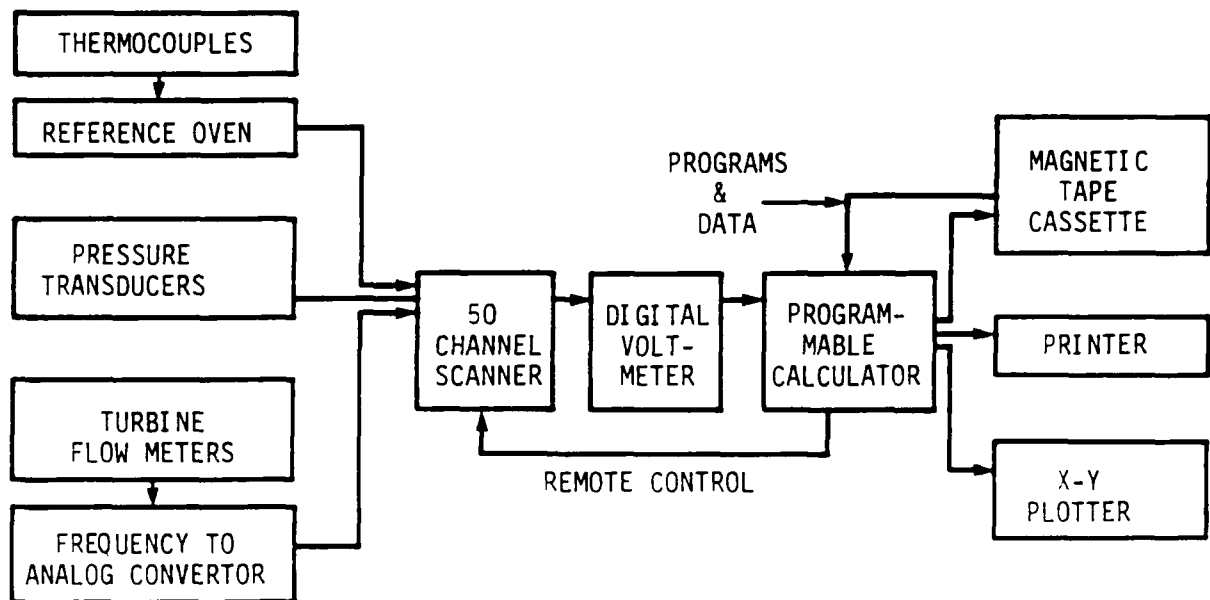
Figure 7. <u>Data acquisition system</u>

systems and then feeds the corresponding digital values to the calculator. The calculator handles all of the data reduction and any necessary calculations, e.g., combustion efficiency, flow factor, and exhaust emissions coefficients. The resulting data are then processed in one of three ways:

1. The data can be sorted on magnetic tape for further reduction at a later time;

2. The data can be output graphically on an X-Y plotter, or

3. The data can be output on a printer along with any appropriate alphanumeric titles or column headings.

E. Spark Gap Measurements

Ignition is believed to occur within a spark kernel in the vicinity of the spark gap. In this region, the conditions including gas velocity, fuel/air ratio, and spark energy are essential in modeling the ignition process. In the present study, the gas velocity and fuel/air ratio in the T63 combustor were measured in the region of the spark gap. Spark energy was maintained constant.

1. Gas Velocity

Flow measurements in the combustor were made at a position of 1.6 mm (0.063) inches away from the spark igniter tip using a hot-film anemometer probe. Fig. 8 is a schematic of the probe installation in the combustor. An igniter was modified to accommodate the hot-film anemometer probe. Basically, the probe replaced the inner electrode of the igniter. A stainless steel tube was used to house the probe.
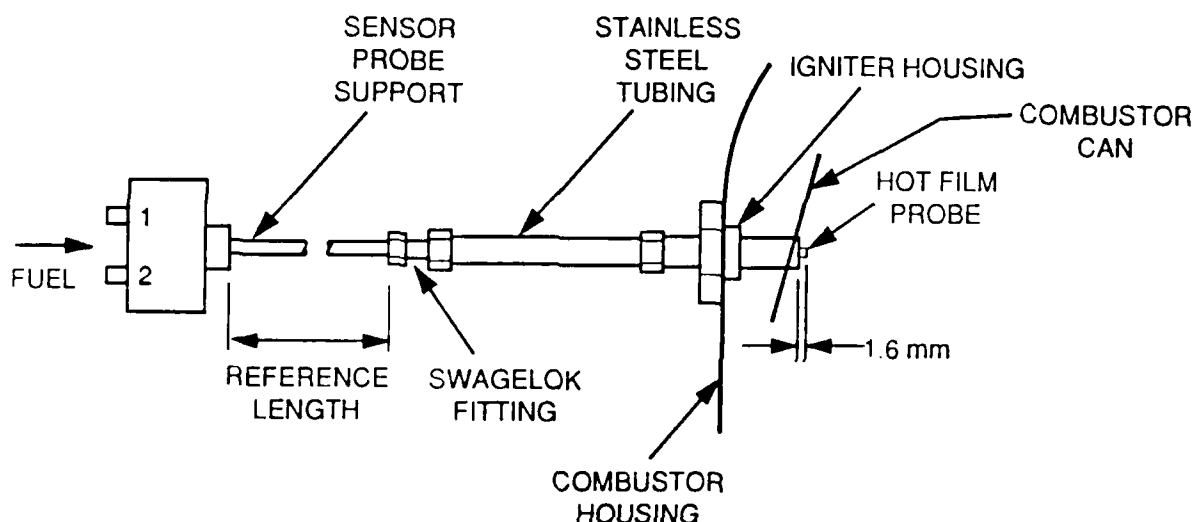
Figure 8. Schematic of hot-film anemometer probe installation in T63 combustor

2. Fuel/Air Ratio

The fuel/air ratio at the spark gap was determined with a heated gas sampling probe (0.125 inch ID) located about 1.6 mm (0.063 in.) from the igniter tip into the gas stream. The liquid fuel droplets that entered the probe were rapidly vaporized in a heated sample line leading to a copper oxide/platinum oxidation catalyst. The inlet flow rate into the probe was very small compared to the combustor inlet airflow; it was not expected to significantly perturb the flow in the region of the spark gap. The catalyst shown in Fig. 9 was used to oxidize the fuel/air mixture to CO, CO_2, and water. Preliminary measurements were made to confirm satisfactory operation of the catalytic oxidation unit. Near stoichiometric mixtures of heptane vapor in air were passed through the catalytic unit, and the products were analyzed using nondispersive infrared for CO and CO_2 and a hydrocarbon analyzer for total

STAINLESS STEEL
BAR STOCK

HEATED SAMPLE INLET LINE

TO PROBE

+ CARTRIDGE HEATER
−

THERMOCOUPLE

TO CO, CO2, THC, AND O2 ANALYZERS

PLATINIZED ASBESTOS/COPPER
OXIDE WIRE MIXTURE

MOUNTING BRACKET
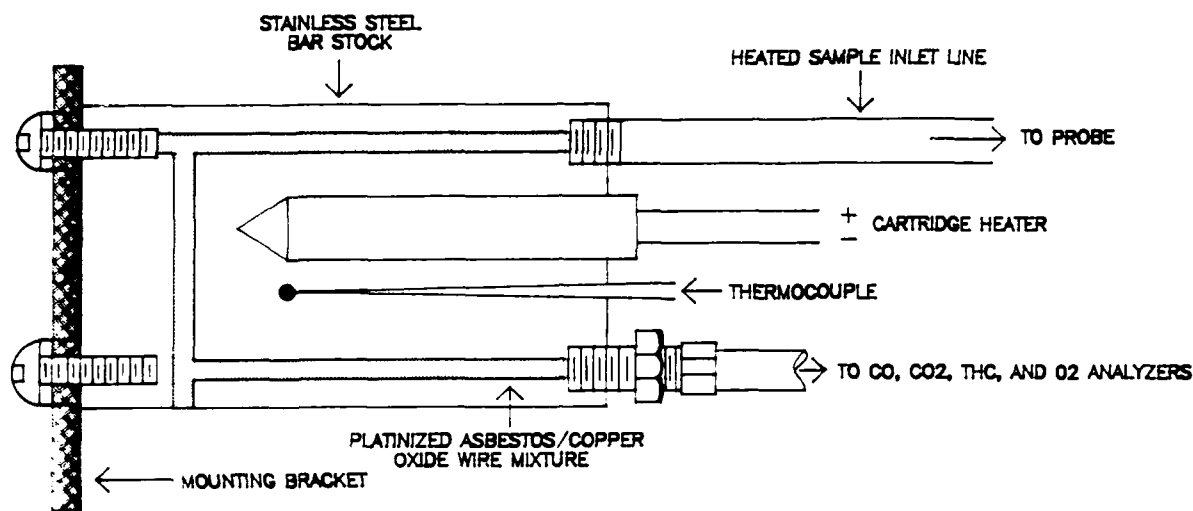
**Figure 9. Oxidation catalyst system used to determine
fuel/air ratio at the spark gap**

hydrocarbons, THC. A lab analyzer was used to measure excess oxygen in the products. With a catalyst temperature ranging from 350° to 400°C, the conversion of fuel carbon to CO and CO_2 was found to be about 99 percent. When rich mixtures were oxidized, the products contained higher concentrations of CO and THC. The fuel/air ratio was calculated from the concentrations of CO, CO_2, O_2, and THC according to the method described by Hardin.(23)

F.   High-Speed Camera and Periscope

For photographing ignition and flame stability phenomenon, the T63 combustor rig was interfaced with a periscope, fabricated according to BFLRF specification. As shown in Fig. 10, the periscope was placed in the exhaust section of the rig at a position such that it could focus on the atomizer and igniter in the dome of the combustor. To create optical access, a window was placed in the center body located in the exit plane of the combustor; the center body is an integral part of the combustor used to divert burned gases into the turbine inlet section of the engine. A Hycam camera with a C-lens mount was used with the periscope to take high speed (up to 2000 frames/s) pictures of the ignition process. The camera speed was

16
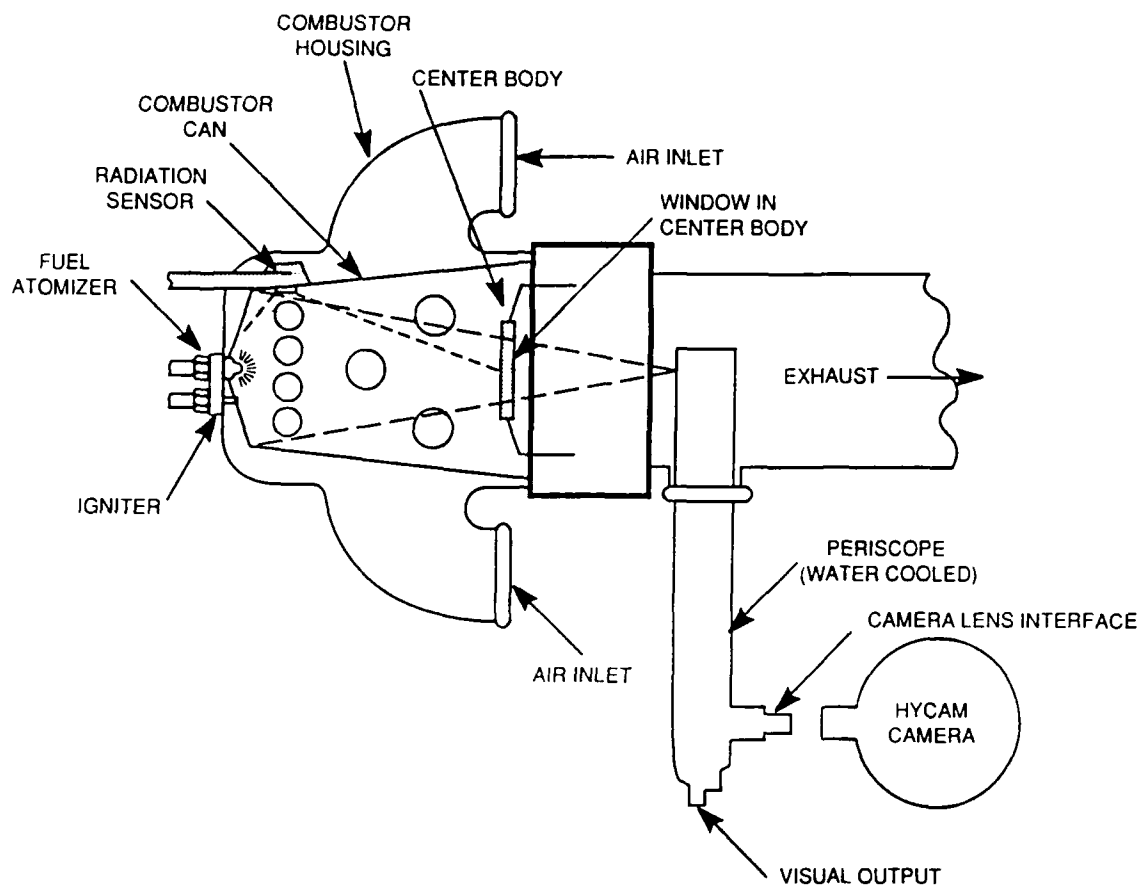
Figure 10. High-speed camera and periscope for photography of ignition process in T63 combustor

limited by the visible radiation produced by the ignition kernel and the diffusion flame that indicated ignition.

G. Test Fuels

The test fuels described in TABLE 1 were chosen for the ignition study because of their broad range of viscosities, volatilities, and chemical compositions. Fuels 1 through 8 were used to investigate the effects of viscosity and volatility on cold start ignition. Fuels 1, 9, and 10 were used to examine the effects of aromatic content on the ignition process. In order to independently study the effects of viscosity and volatility on the ignition process, Fuel 4 was blended with a viscosity equal to that of JP-5 and a front end boiling point distribution similar to JP-4. Fuel 5 was blended with a viscosity equal to that of JP-4 and a front end boiling point distribution similar to gasoline. The viscosities of gasoline and methanol are essentially the same, but their 10 percent boil-off temperatures and heats of

TABLE 1. Fuel Properties

Fuel No.	Fuel Description	Specific Gravity	Vis (cSt)	Surface Tension (dynes/cm)	10% Boil-Off Temperature (°C)	H/C Atom Ratio	Arom (wt%)
1	JP-8	0.8236	2.51	27.18	169.4	1.90	19.8
2	JP-4	0.7519	1.22	24.29	98.0	2.01	--
3	JP-5	0.8080	3.48	27.02	189.2	1.93	--
4	NDF/25% Gasoline	0.8265	3.61	27.01	112.2	1.80	--
5	NDF/70% Gasoline	0.7839	1.32	24.01	36.1	1.81	--
6	NDF	0.8484	7.85	28.79	209.9	1.79	--
7	Methanol	0.7913	1.03	22.44	65.0	4	0
8	Gasoline	0.7555	0.90	21.89	16.6	1.82	--
9	JP-8/50% Aromatic Blend	0.8554	2.59	--	168.1	1.63	54.9
10	Aromatic Blend	0.8960	2.66	--	165.2	1.39	90.8

vaporization are very dissimilar. Fig. 11 illustrates the relationships between the 10 percent boil-off temperature and the viscosity of Fuels 1 through 8.

The effect of chemical composition was examined because some studies have indicated that fuels with high aromatic content exhibit longer ignition delays and thus require greater fuel/air ratios for ignition. The objective in blending Fuels 9 and 10 was to allow variation in the aromatic content while maintaining the viscosity and volatility the same as that of JP-8. Fuel 10 is a blend of 84 percent heavy aromatic naphtha and 16 percent xylene bottoms; it is 90.8 percent aromatics, and its viscosity and front-end boiling-point distribution are essentially the same as JP-8. Fuel 9 is a 50/50 blend of JP-8 and Fuel 10.
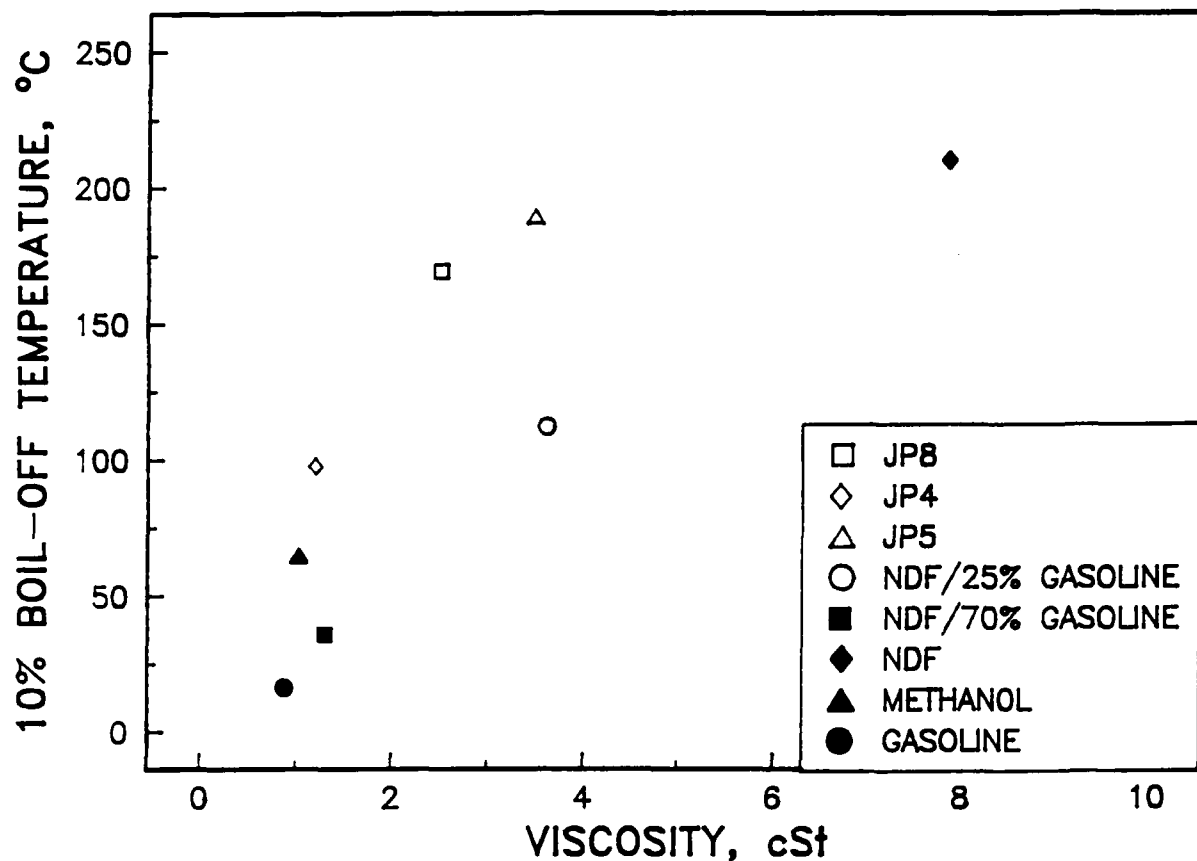
Figure 11. **Viscosities and volatilities of fuels 1 through 8**

H. Droplet-Size Measurement

Atomization is of critical importance to the ignition of fuel sprays in gas turbine engines. Degraded atomization is caused, for the most part, by increased fuel viscosity; as a result, more viscous fuels and lower fuel temperatures lead to higher fuel/air ratio requirements for ignition. It is a general rule that when fuel viscosities exceed 12 cSt combined with lower burner inlet air temperatures, gas turbine engines become more difficult to ignite at any fuel/air ratio. Ignition failure occurs with degraded atomization because of the decreased fuel surface area available for evaporation and the increased spark energy required for droplet evaporation.

To better understand the ignition test results in the T63 combustor, droplet-size measurements were made on hollow cone sprays produced by the atomizers described in TABLE 2.

TABLE 2. Fuel Atomizers

Description	Nominal Capacity (gal./hr)	Actual Capacity* (gal./hr) @ 100 psid)	Flow Number* $(kg/s \cdot \sqrt{Pa})$	Cone Angles (degrees)
Factory T63 Dual Orifice Pressure Swirl	-	6.98^+	7.14×10^{-6}	--
Delavan Simplex Pressure Swirl	4	3.74	3.83×10^{-6}	90
Delavan Simplex Pressure Swirl	5	4.72	4.83×10^{-6}	90
Delavan Simplex Pressure Swirl	6	6.04	6.18×10^{-6}	90
Delavan Simplex Pressure Swirl	7	6.92	7.08×10^{-6}	90
Delavan Simplex Pressure Swirl	8	8.24	8.43×10^{-6}	90

* Capacity and flow number for JP-5.
+ Primary nozzle only.

The standard T63 atomizer is a dual orifice nozzle that uses a flow divider valve internal to the nozzle body to determine the fuel flow split between the primary and secondary nozzles. The flow divider valve responds to pressure rather than mass flow rate. At low flow rates, such as those used in ignition, the valve completely restricts the flow of fuel through the secondary nozzle. As a result, the droplet-size measurements were made only on sprays originating from the primary nozzle.

The standard T63 atomizer is also equipped with a passage way to carry burner inlet air through the nozzle. The airflow is used to prevent deposit buildup on the nozzle face exposed to combustion gases. However, the airflow was also found to affect the droplet-size distribution and, therefore, had to be accounted for in the measurement technique. To simulate this airflow, a special manifold was designed to allow the separate flows of fuel and air through the atomizer.

All the Delavan atomizers were single-orifice pressure-swirl (simplex) nozzles differing only in flow rate capacity. Compared to the standard T63 atomizer, the droplet-size measurements in sprays from the Delavan atomizers were relatively straight forward.

The test fluids used in the atomization measurements included JP-4, JP-5, NDF, a heavy marine gas oil (HMGO), and HMGO cooled to 274K. The first three of these fluids are described in TABLE 3 the test fuels section; HMGO is a heavy marine gas oil selected because of its relatively high viscosity. The test fluids and test conditions used in the atomization measurements are given in TABLE 3. The flow rates ranged from 1 to 7 g/s depending on the atomizer and fuel combination examined.

TABLE 3. Test Fluids for T63 Ignition/Atomization Study to Generate the Correlation for Sauter Mean Diameter (SMD) with Fuel Properties and Flow Conditions

Fluid	Test Temp (K)	Kinematic Viscosity at Test Temp (cSt)	Surface Tension at Test Temp (dynes/cm)	Density at Test Temp (g/mL)
JP-4	298	0.85	23.9	0.746
JP-5	298	2.02	26.6	0.801
NDF	298	3.77	28.4	0.841
HMGO	298	9.8	31.1	0.868
HMGO (Cold)	274	29	33.3	0.884

Drop-size data were obtained with a particle sizer based on the diffraction angle produced by drops when illuminated by a collimated beam of mono-chromatic, coherent light from a HeNe laser. A 300-mm focal length f/7.3 lens was used to collect the scattered light. The laser beam diameter was 9 mm with a Gaussian intensity distribution truncated at the edge by the 9-mm aperture. Data were recorded at an axial distance of 38.1 mm (1.5 in.) downstream of the nozzle tip.

Two procedures were necessary to ensure the proper calibration of the particle sizing instrument. The drop-size distribution is computed from the relative scattered light intensity measured at different scattering angles by a set of 30 annular ring photodiodes. For an ideal optical and electronic system and uniform responsivity between photodiodes, the signal intensity may be used to compute the drop-size distribution without resorting to external calibration standards. Tests at this laboratory have shown that the nonidealities of the system are negligible except for the detector responsivities that must be determined for each instrument in order to get accurate results. This was the first procedure, described by Dodge (24), developed specifically to assure proper calibration of the system.

The second procedure was necessary to correct for the very dense (optically) fuel sprays obt_ined at the higher fuel flow rates. In the standard configuration, the instrument monitors the unscattered laser beam intensity with a photodiode mounted on the centerline of the optical system. The instrument instruction manual indicates that if the scattered light intensity exceeds the unscattered light intensity, a significant number of photons are being scattered by more than one drop. Since the theory relating scattered light intensity to drop-size assumes diffraction by a single drop, these multiple-scattered photons will result in errors in the computed size distribution. In order to evaluate the problem and develop correction procedures, experiments have been conducted at this laboratory (25) and another.(26) This second procedure (26) was used in only a few instances to correct the data recorded when dense sprays were encountered.

All tests were performed at atmospheric conditions in a test chamber of square cross-section 30 cm on a side and 76 cm long, with air pulled through the chamber at a velocity of about 2.1 m/s by an explosion-proof exhaust fan. A set of twisted metal screens in the exhaust duct removed the fuel mist from the air before exhausting to the atmosphere.

Fuel pressures were measured with a 150-psia pressure gauge and a 500-psig gauge. Flow rates were measured volumetrically by collecting the spray in a graduated cylinder.

All spray data were reduced assuming a Rosin-Rammler drop-size distribution, which is specified by two parameters X and N, defined by,

$$R = \exp\left(-\left((D/X)^N\right)\right) \tag{8}$$

where R is the cumulative volume (or mass) fraction of the spray contained in drops whose diameters are larger than D. Thus X is a size parameter, in micrometers, and N indicates the width of the distribution. Large values of N imply narrow distributions and vice versa. Fuel sprays are usually characterized by an "average" size based on the volume-area mean diameter ($\bar{D}_{32}$), more commonly called the Sauter Mean Diameter (SMD), defined by (27)

$$SMD = \bar{D}_{32} = \frac{\Sigma_i \, D_i^3 \, N_i}{\Sigma_i \, D_i^2 \, N_i} \tag{9}$$

where D_i is the drop diameter and N_i is the population of drops in the size class D_i. The SMD is a mean diameter that represents a fictitious spray composed of drops of uniform size having the same total drop surface and volume as the actual spray. The SMD is computed from the Rosin-Rammler parameters by (27),

$$SMD = X / \Gamma(1-1/N) \tag{10}$$

where Γ is the gamma function.

IV. RESULTS AND DISCUSSION

The purpose of this study was to examine the assumptions used in the characteristic time model and gain a more basic understanding of the ignition process in gas turbine engines. The results of this work are presented as five basic parts. The first part includes the relatively fundamental measurements of gas velocity and fuel/air ratio at the spark gap. The second part is a discussion of the high-speed filming of the ignition process showing the creation of the ignition kernel, the dark induction period, and the start of flame propagation. The third part describes the measurement of average drop sizes (as determined by SMD) of sprays from the six atomizers used in the ignition measurements and the correlation of SMDs with atomizer flow conditions and fuel properties. In the fourth part, the actual ignition measurements are presented; also, the effects of combustor flow conditions, fuel properties, and SMDs on the limiting fuel/air ratio are examined. In the fifth and final part, characteristic time calculations are presented for the data, and the validity of the model is examined.

A. Spark Gap Measurements

To aid in understanding the ignition mechanism and to justify some of the assumptions used in the characteristic time model (CTM), the gas velocity and fuel/air ratio were measured at the spark gap. Fig. 12 shows the correlation of the gas velocity at the spark gap with the reference velocity through the combustor. The velocity measurements were made with a hot film anemometer probe placed about 1.6 mm away from the electrode of the igniter. It is seen in Fig. 12 that the velocity near the spark gap is about an order of magnitude lower than the reference velocity. However, as assumed in previous CTM studies, the velocity at the spark gap is essentially proportional to the reference velocity. The correlation given below will be used in the CTM computer code to calculate the velocity at the spark gap in terms of the reference velocity,

$$V_{sg} = -0.0138 + 0.010225 V_{ref} - 1.042 \times 10^{-3} V^2_{ref} \qquad (11)$$

The fuel/air ratio at the spark gap was also measured about 1.6 mm away from the igniter. The fuel/air mixture, mostly fuel droplets and some vapor, was drawn into

24
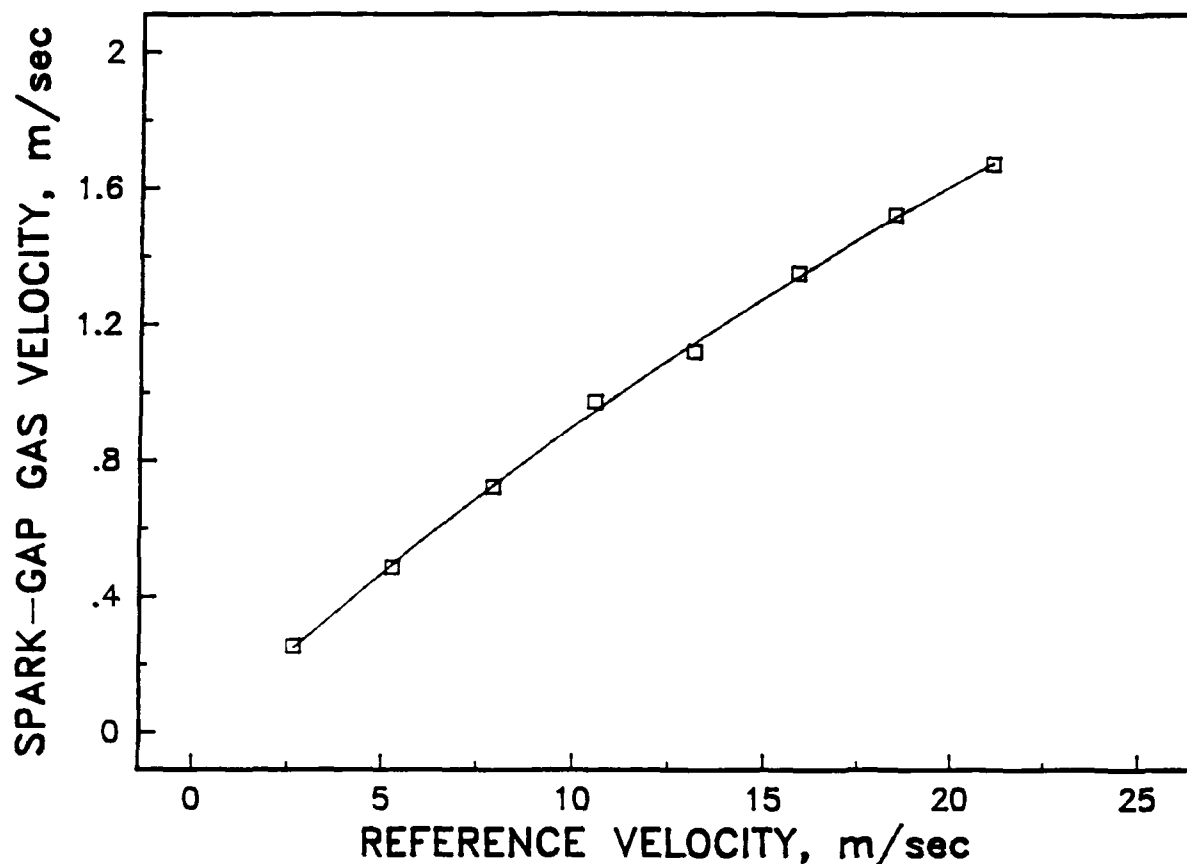
Figure 12. Correlation of gas velocity at the spark gap with the reference velocity through the combustor

the probe, vaporized, and analyzed. Figs. 13 and 14 show the effect of overall fuel/air ratio in the combustor on the fuel/air ratio at the spark gap for JP-4 and JP-8 at the three reference velocities used in the ignition measurements.

The results show that the fuel/air ratio at the spark gap remains essentially constant over a wide range of overall fuel/air ratios. For the 5 m/s reference velocity, the fuel/air ratios at the spark gap are slightly below the stoichiometric fuel/air ratio, but still well above lean limit. At the higher reference velocities, the fuel/air ratios at the spark gap are greater than the stoichiometric fuel/air ratio.

In previous studies (14), little or no correlation of the ignition data using the CTM calculations was obtained unless the equivalence ratio at the spark gap was
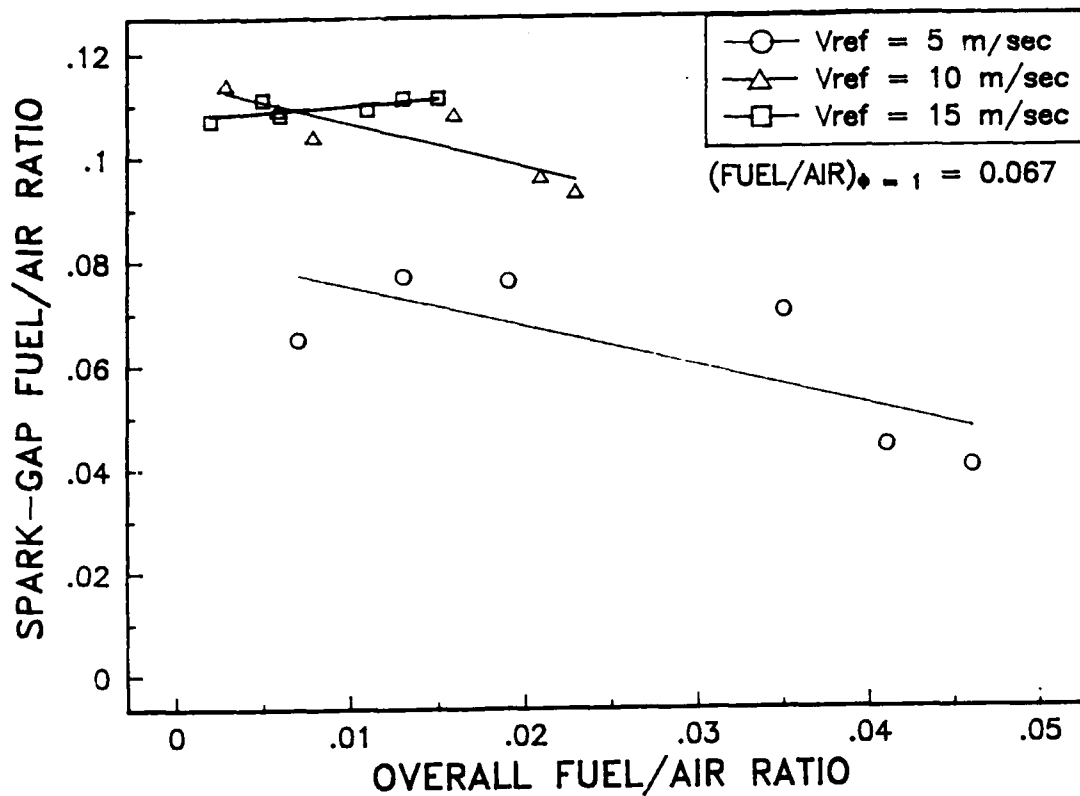
Figure 13. Fuel/air ratio (liquid plus vapor) at the spark gap versus overall fuel/air ratio for combustor, JP-4 fuel
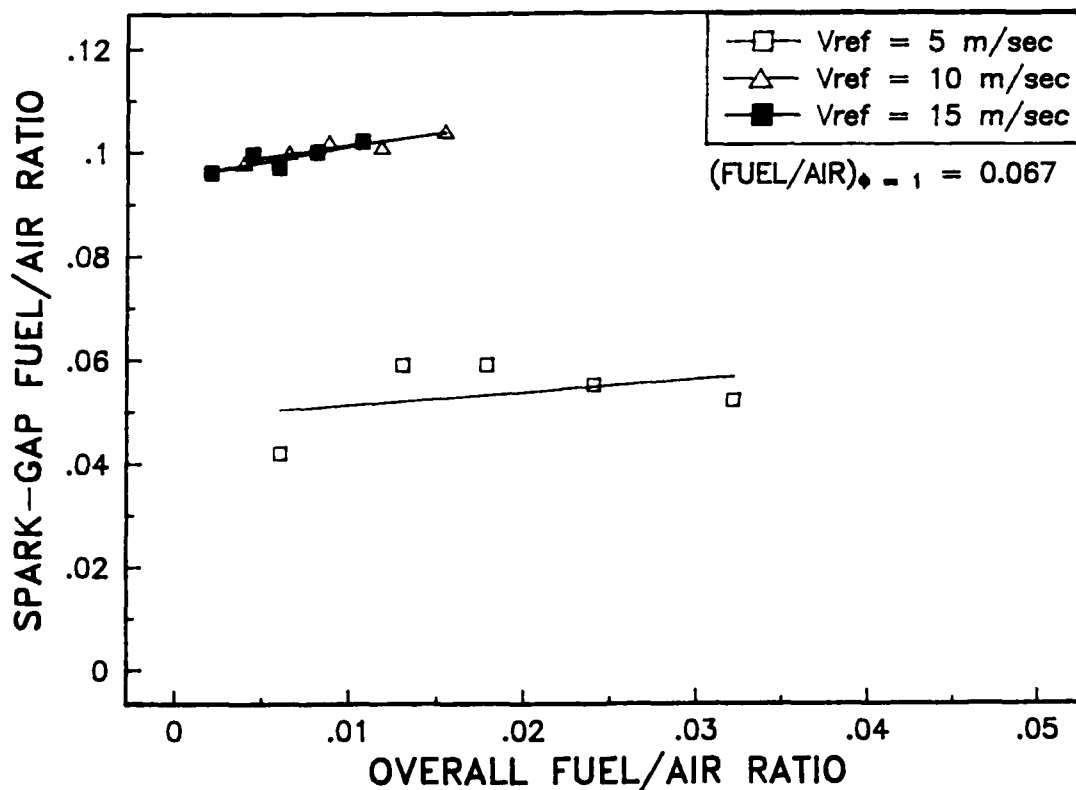
Figure 14. Fuel/air ratio (liquid plus vapor) at the spark gap versus overall fuel/air ratio for combustor, JP-8 fuel

assumed to be a constant. In view of the measurements presented here, the assumption that the equivalence ratio at the spark gap is a constant now appears to be a reasonable approximation.

B. Ignition Delay Measurements

High-speed photographs of the ignition event were acquired with a Hy-Cam camera interfaced with a periscope device mounted on the T63 combustor rig. The photos were taken at speeds of 250, 500, 1000, and 2000 frames per second, but 1000 frames per second appeared optimum. The fuels examined included JP-4, JP-8, NDF, and the high aromatic blend, Fuel 10. Fig. 15 is an artist's conception of what was typically observed in the high-speed photographs. Unfortunately, it was not possible to obtain acceptable editorial quality in processing the photographic data.
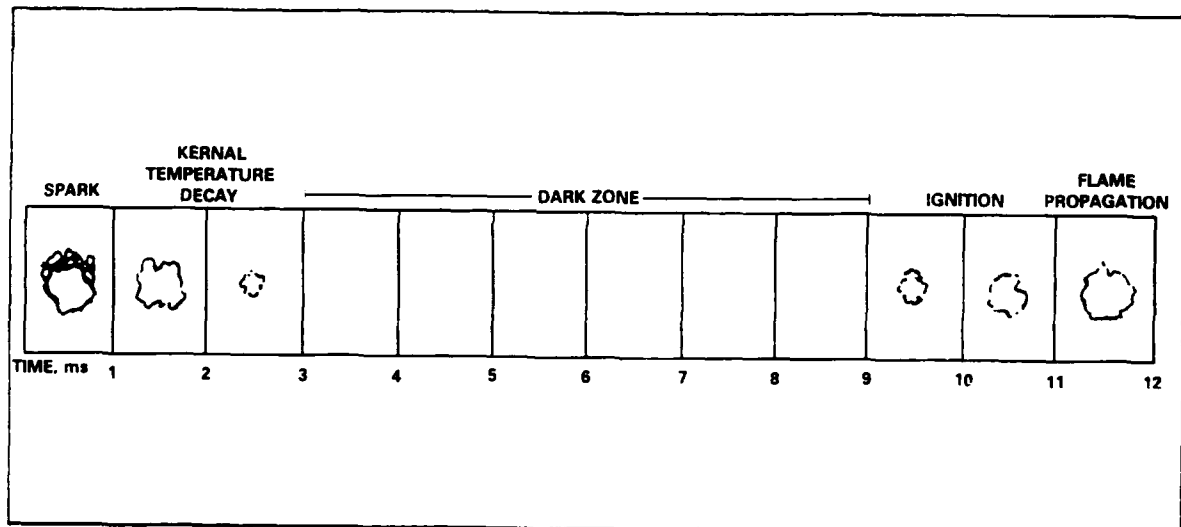
Figure 15. Artist's conception of the high-speed photographs of
the ignition phenomenon in the T63 combustor

In the first frame of each ignition event, a relatively bright kernel was produced by the spark. In some of the pictures, there was some weak light emission from the kernel that decayed rapidly in the next two frames. In the next 5 to 10 frames, there appeared to be a dark zone that showed no visible evidence of combustion. Depending to some extent on the fuel, flame radiation began to appear about 8 to 13 ms after the spark. Based on these observations, it was concluded that the ignition delay time occurred after the dark zone when flame radiation became visible.

There was no discernible variation in the ignition delays of JP-8, JP-5, NDF, and the high aromatic naphtha, Fuel 10, but the ignition delay for JP-4 appeared to be a few milliseconds shorter than the other fuels. Since JP-4 is a more volatile and less viscous fuel, it is not surprising that it would be more finely atomized and would evaporate more rapidly.

The results of this study show that the ignition delay is quite long, ranging from 8 to 13 ms. The fact that there is a dark zone lasting for most of the ignition delay indicates that the temperature within the ignition kernel during the droplet evaporation process (dark zone) is substantially less than the stoichiometric adiabatic flame temperature. This observation may greatly influence efforts to model ignition in gas turbine combustors since, in previous work employing the CTM analysis, it was assumed that the temperature within the spark kernel was equal to the stoichiometric flame temperature.

C. Droplet-Size Results

Ignition in gas turbine engines is strongly dependent on fuel atomization because it is the droplet size that determines the rate of fuel vaporization. The Sauter Mean Diameter (SMD) of the spray depends on the atomizer, fuel properties, and the flow conditions within the combustor. Atomizers are developed to produce fast evaporating sprays at various flow conditions within the combustor. Usually the atomizers are designed with staged primary and secondary fuel nozzles; the primary is used to produce a fine spray mainly for ignition and altitude relight while the secondary forms a coarser high volume spray that fuels the higher power operating conditions. Fuels have different ignition characteristics in gas turbine combustors because fuel properties such as viscosity and surface tension have significant effect on the atomization process. In the present study, SMDs were measured in fuel sprays produced by the standard T63 dual-orifice pressure-swirl atomizer and five Delavan simplex atomizers at several flow rates using five test fluids (see TABLE 4).

The SMDs of the sprays were measured at several fluid flow conditions with a laser-diffraction particle sizer. The measurements were made along the centerline of the spray about 38 mm from the nozzle tip. The SMD obtained by this approach was basically an average through the spray centerline; no account was taken of the

radial drop-size distribution in the spray. Fig. 16 shows the effect of the fuel flow rate on the SMD for all the atomizers examined. Clearly, the results show that the capacity of the atomizer has a significant effect on the flow rate required to achieve a desired SMD. It is found that for a given fuel flow rate, the measured SMD decreases markedly as the capacity (or flow number) of the atomizer is reduced. By inspection of Fig. 16, it can be seen that the SMD is reduced by approximately a factor of two by changing from a 7-gal./hr atomizer to a 4-gal./hr atomizer.
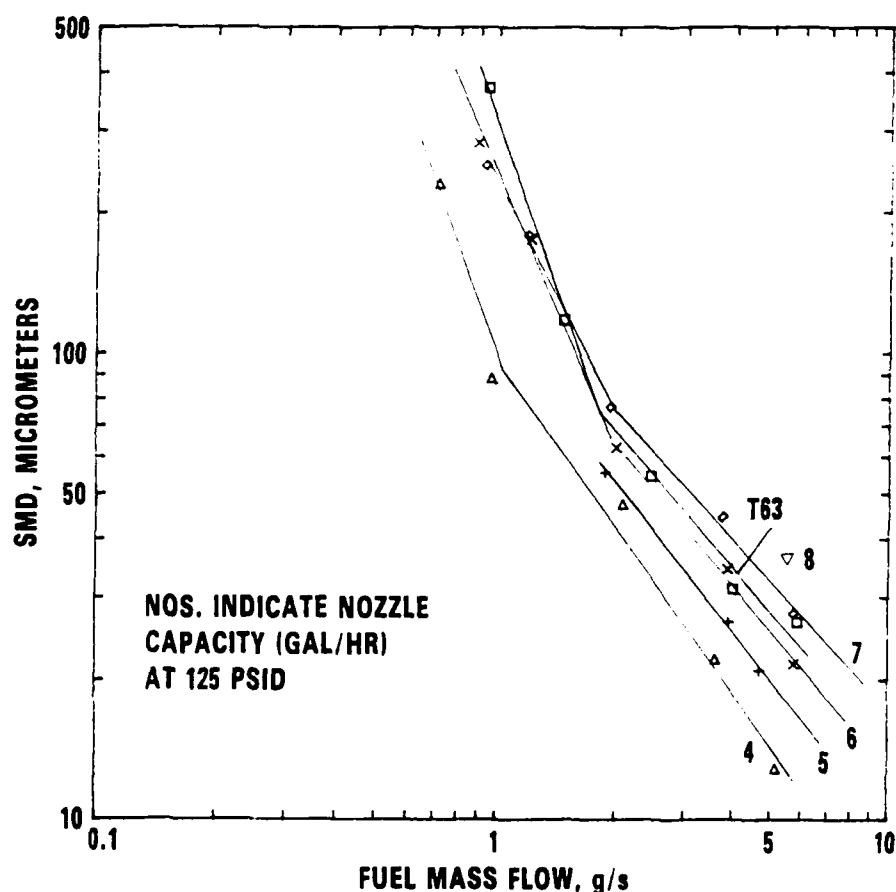
Figure 16. Effect of fuel flow rate and nozzle capacity on SMD

The break in the curves at low fuel flow rates shown in Fig. 16 is probably due to the Weber number effect observed by Simmons and Harding.(28) The Weber number, We, is the ratio of inertial forces to the surface tension forces. The SMD is much

more dependent on flow rate when We < 1, i.e., at lower flow rates. This effect was not important in the present study because it was found that the minimum fuel flow rates for ignition always occurred at We > 1 for these atomizers.

Fig. 17 shows the effect of fuel type on the SMDs measured in sprays produced by the T63 atomizer. The results show that fuel properties have a significant effect on the SMD/mass flow rate correlations. The fuel effect is most pronounced for HMGO at ambient temperature and 274K. Otherwise, the JP-4, JP-5, and NDF fuels tested in the high mass flow rate regime (We > 1) gave very similar SMDs. Considering the fuel properties in TABLE 3, it is apparent that the dramatic increases observed in the SMDs of HMGO are most probably attributed to increased viscosity.

Figs. 18 and 19 show the fuel effects on SMDs measured in sprays produced by Delavan simplex atomizers with capacities of 4 and 6 gal./hr, respectively. Compared to the standard T63 atomizer, the fuel effects on SMD appeared to be more pronounced in sprays produced by the Delavan atomizers. This fuel effect was especially apparent among the JP-4, JP-5, and NDF fuel sprays generated at the higher mass flow rates that were used in the actual ignition studies. The fuel effects on SMDs produced by the 5-, 7-, and 8-gal./hr Delavan simplex atomizers were similar to those shown in Figs. 18 and 19.

Atomization Correlations - The five Delavan simplex atomizers with different flow capacities performed similarly, with the larger capacity nozzles producing larger drop sizes at equivalent conditions. The average drop size as represented by the Sauter mean diameter (SMD) could be correlated with the fuel nozzle capacity (flow number), the fuel flow rate, and the fuel viscosity and surface tension as follows:

$$SMD = 4.052 \, FN^{1.18} \nu^{0.212} \sigma^{0.457} \dot{w}_f^{-1.16} \qquad (12)$$

where SMD = Sauter mean diameter, micrometers

ν = Viscosity, cSt

σ = Surface tension, dynes/cm

FN = Flow number, kg/s - $\sqrt{Pa}$ x 10^6

$\dot{w}_f$ = Mass flow rate, g/s
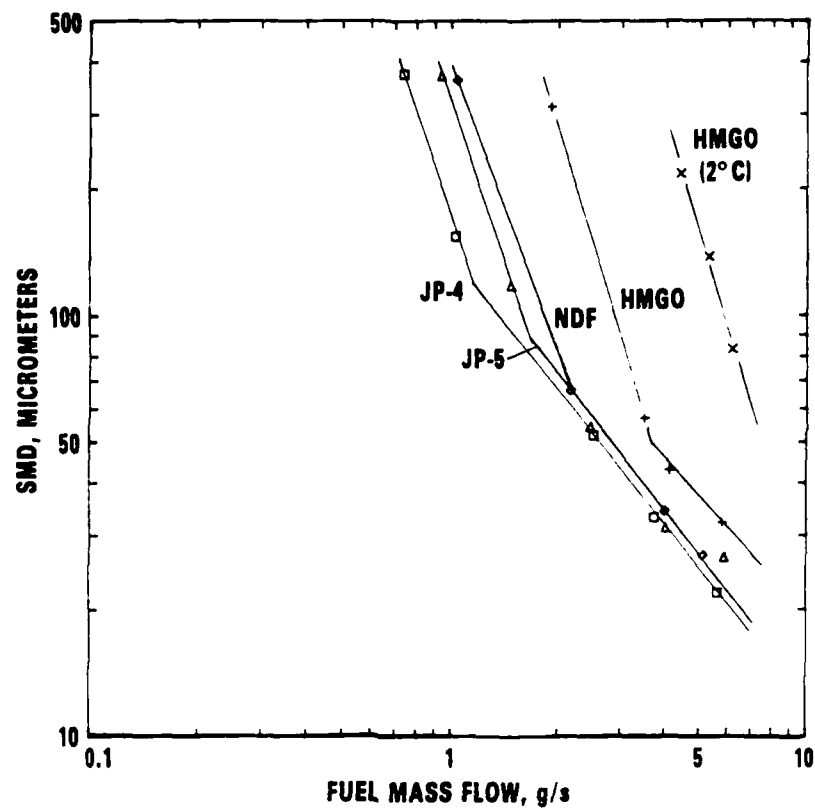
Figure 17. Effect of fuel flow rate and fuel type on SMD produced by the standard T63 atomizer
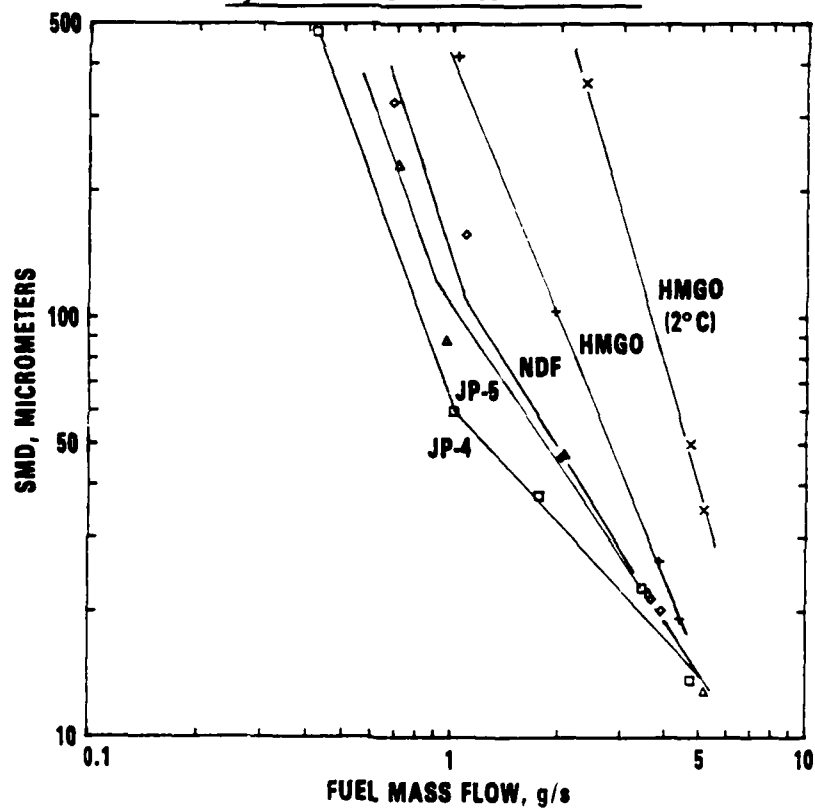
Figure 18. Effect of fuel flow rate and fuel type on SMD produced by the Delavan 4 gal./hr atomizer

31
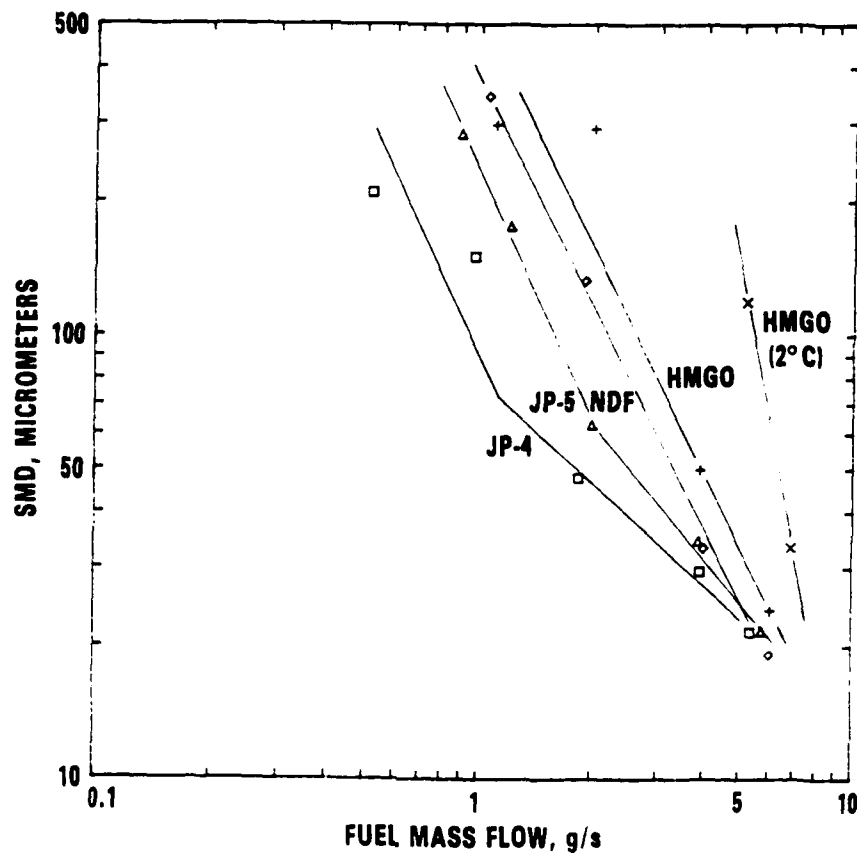
Figure 19. Effect of fuel flow rate and fuel type on SMD produced by the Delavan 6 gal./hr atomizer

The standard T63 atomizer performed similarly, but had an additional complication due to airflow used across the nozzle face to reduce carbon buildup. This airflow had to be accounted for in the SMD measurements because it had a small effect on the atomization process. The ignition tests in the T63 combustor were performed at three airflows, 91, 182, and 273 g/s. The atomization characteristics of the T63 atomizer were measured at pressure drops corresponding to the 91 and 273 g/s conditions, with the atomization at the intermediate condition assumed to be the average of the two extremes. The SMD correlation at the 91 g/s airflow condition for the T63 atomizer was,

$$SMD = 112.6 \, \nu^{0.399} \, \dot{w}_f^{-1.21} \qquad (13)$$

and at the 273 g/s airflow condition,

$$SMD = 99.7 \, \nu^{0.334} \, \dot{w}_f^{-1.09} \qquad (14)$$

32

Eqs. (12) through (14) were used to calculate SMDs of fuel sprays at the ignition limits in the T63 combustor. These calculated SMDs were used in the following sections of this report to ascertain the effects of atomization on the ignition process in a gas turbine engine.

D. Cold-Start Ignition

Cold-start ignition experiments were conducted at several operating conditions in a T63 combustor rig; TABLE 4 shows the range of test conditions used. To simulate a sea-level start, pressures were kept close to one atmosphere. Burner inlet temperatures were varied from ambient to -34°C (-29.2°F). The mass flow rate of air was varied to change the reference velocity in the combustor. Fuel temperature was varied in order to examine the effects of viscosity, surface tension, and the SMD of the spray on the limiting fuel/air ratio for ignition.

TABLE 4. Combustor Operating Conditions for Ignition

Pressure, kPa: 103 to 124

Burner Inlet Temperature, °C: 25, 10, 0, -24, -34

Fuel Temperature, °C: 0 to 30

Mass Flow Rate, kg/s: 0.09, 0.18, 0.27

Reference Velocity, m/s: 5, 11, 16

Six atomizers including the standard T63 atomizer and five Delavan atomizers were used in the tests to determine the effects of droplet size and spray structure on the limiting fuel/air ratio for ignition.

The ignition limits of the test fuels were measured in terms of the overall fuel/air ratio required to achieve ignition at a given set of operating conditions. These tests were performed by first establishing the desired airflow conditions in the combustor. The igniter was turned on, and the fuel flow was started at a flow rate below the ignition requirement. The fuel flow was gradually increased, using a motorized valve until ignition occurred. At the point of ignition, the motor turning the fuel valve was stopped, and the minimum fuel flow rate for ignition was recorded.

33

Most of the ignition measurements were made for Fuels 1 through 6 in TABLE 2. Limited data were obtained on methanol and gasoline and Fuels 9 and 10. Fig. 20 shows the effect of reference velocity on the minimum fuel/air ratios for ignition of Fuels 1 through 6 at a fuel and burner inlet temperatures of 300K using the standard T63 dual orifice atomizer. Figs. 21 and 22 show similar results using the 4- and 8-gal./hr Delavan simplex atomizers. The results show that the minimum fuel/air ratio for ignition decreases as the reference velocity increases. This decrease is explained in part by the fact that the mass flow rate of fuel delivered to the atomizer must increase if the fuel/air ratio is to be maintained as the mass flow rate of air through the combustor is increased. When the fuel flow rate is increased, the SMD of the fuel spray decreases and the fuel evaporates more rapidly. It is expected that the minimum fuel/air ratio for ignition should decrease as the SMD of the fuel spray decreases because the drops are more easily vaporized. Another reason that the minimum fuel/air ratio for ignition is higher for 5 m/s reference velocity is that the fuel/air ratio at the spark gap is lower than that measured at the higher reference velocities (see Figs. 13 and 14).

The fuel effects on the minimum fuel/air ratio for ignition are very apparent in Figs. 20 through 22. Fuels such as NDF with high viscosity and low volatility require a higher minimum fuel/air ratio for ignition than the more volatile and less viscous fuels such as JP-4. Fuels with similar viscosities such as JP-8, JP-5, and NDF/25 percent gasoline have similar minimum fuel/air ratios for ignition. It is important to note that the Fuel 4, NDF/25 percent gasoline, was blended with the same viscosity as JP-5, but similar front-end volatility (10 percent pt) to JP-4. Fuel 5, NDF/70 percent gasoline, was blended with the same viscosity as JP-4, but similar front-end volatility to gasoline. By inspection of the data presented in Figs. 20 through 22, it is apparent that Fuel 4, NDF/25 percent gasoline, has a minimum fuel/air ratio for ignition similar to JP-5. Also, Fuel 5, NDF/70 percent gasoline, has a minimum fuel/air ratio for ignition similar to JP-4. The gasoline data are not presented, but its minimum fuel/air ratio, in fact, falls significantly below that of JP-4. These results show that fuels of equal viscosity require similar minimum fuel/air ratios for ignition, and that viscosity appears to be more significant than volatility in the ignition process.
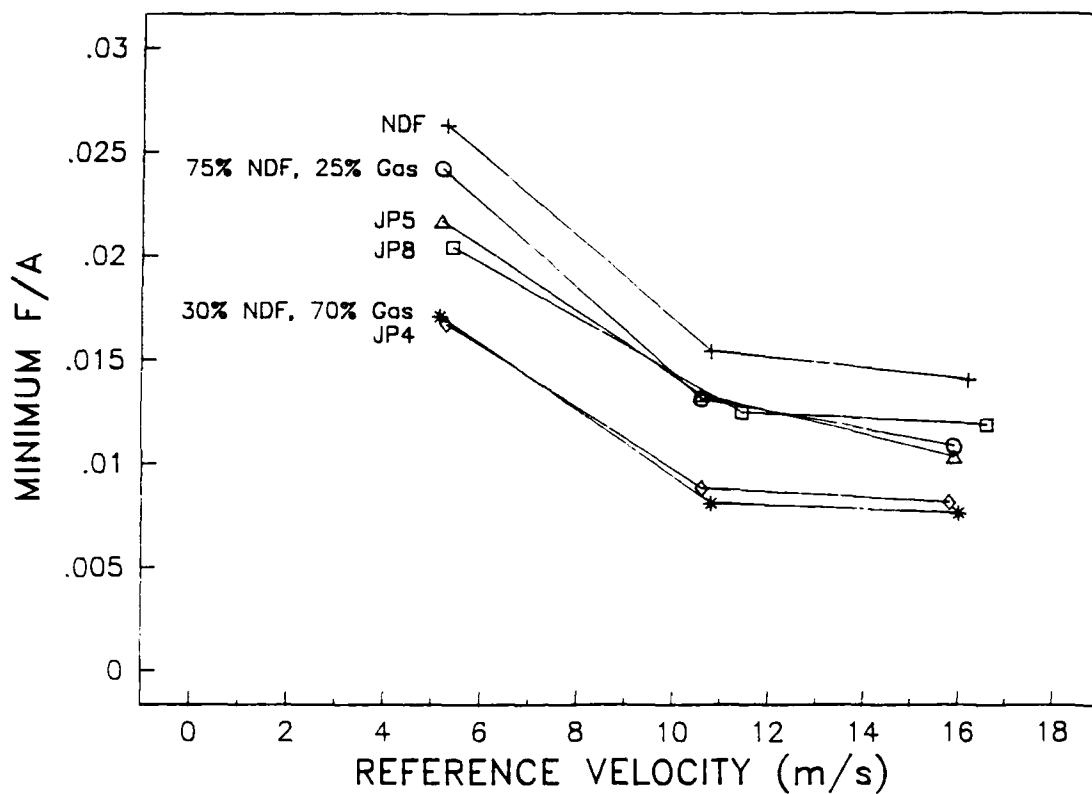
Figure 20. Effect of reference velocity and fuel type on minimum fuel/air ratio for ignition with the standard T63 atomizer
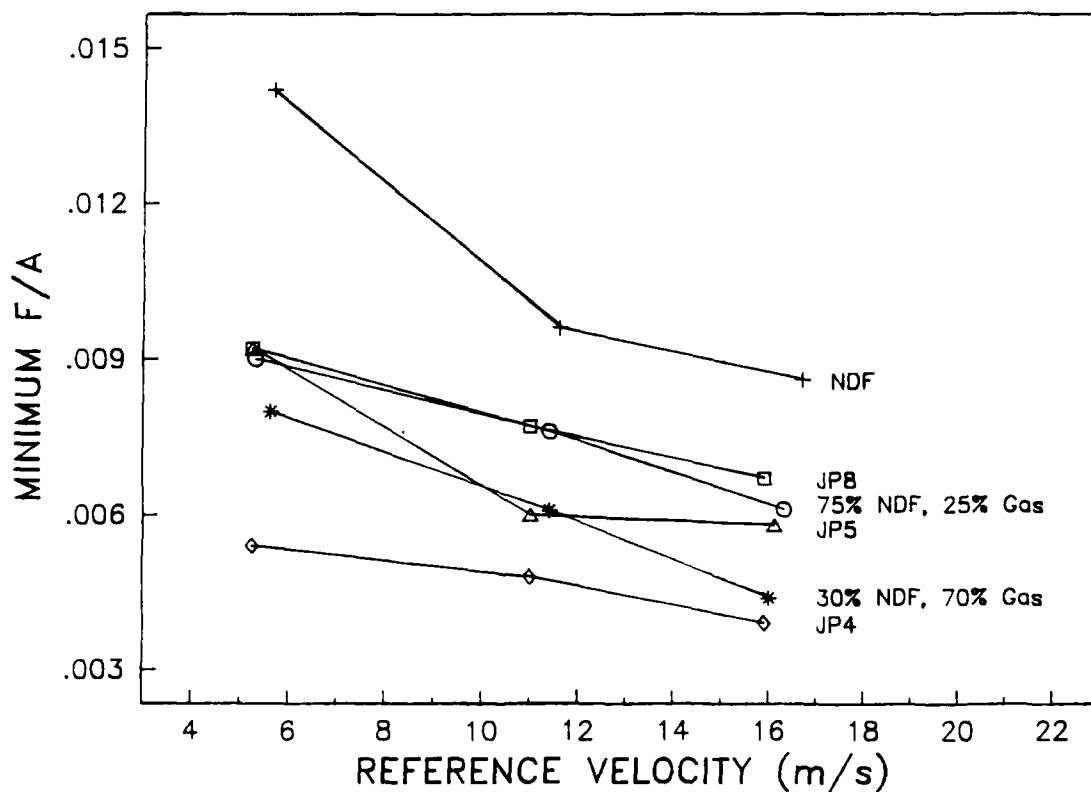
Figure 21. Effect of reference velocity and fuel type on minimum fuel/air ratio for ignition with the Delavan 4 gal./hr atomizer
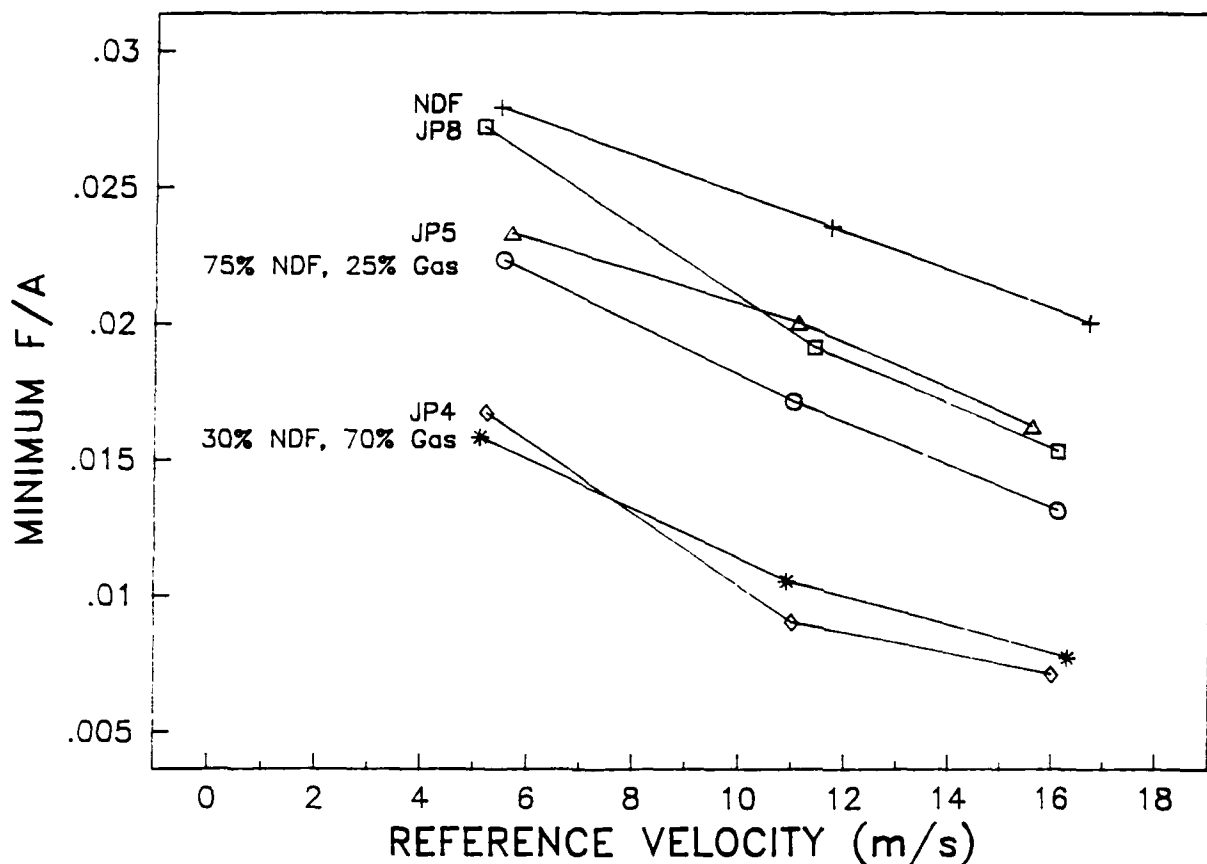
Figure 22. Effect of reference velocity and fuel type on minimum fuel/air ratio for ignition with the Delavan 8 gal./hr atomizer

Figs. 23 through 26 show correlations of the minimum fuel/air ratio for ignition with viscosity and 10 percent boil-off temperature. Figs. 23 and 24 show data obtained with the standard T63 dual orifice atomizer, and Figs. 25 and 26 show data obtained using the 4-gal./hr Delavan simplex atomizer. The results clearly show that the minimum fuel/air ratio correlates more favorably with viscosity than volatility.

The effects of atomization on the minimum fuel/air ratio for ignition have been apparent in the results discussed above. It is evident when comparing the results presented in Figs. 20 through 26 that the minimum fuel/air ratio is much lower for the 4-gal./hr Delavan simplex atomizer than the 8-gal./hr Delavan and standard T63 atomizers. Fig. 27 shows the effect of atomizer flow number on the minimum fuel/air ratio for ignition. The data were measured using JP-5 and a burner inlet temperature of 300K at the 5, 11, and 16 m/s reference velocities. The six points on each line represent the six atomizers employed in this work. If ignition depended only on achieving a critical fuel/air ratio, then Fig. 27 should be a horizontal line
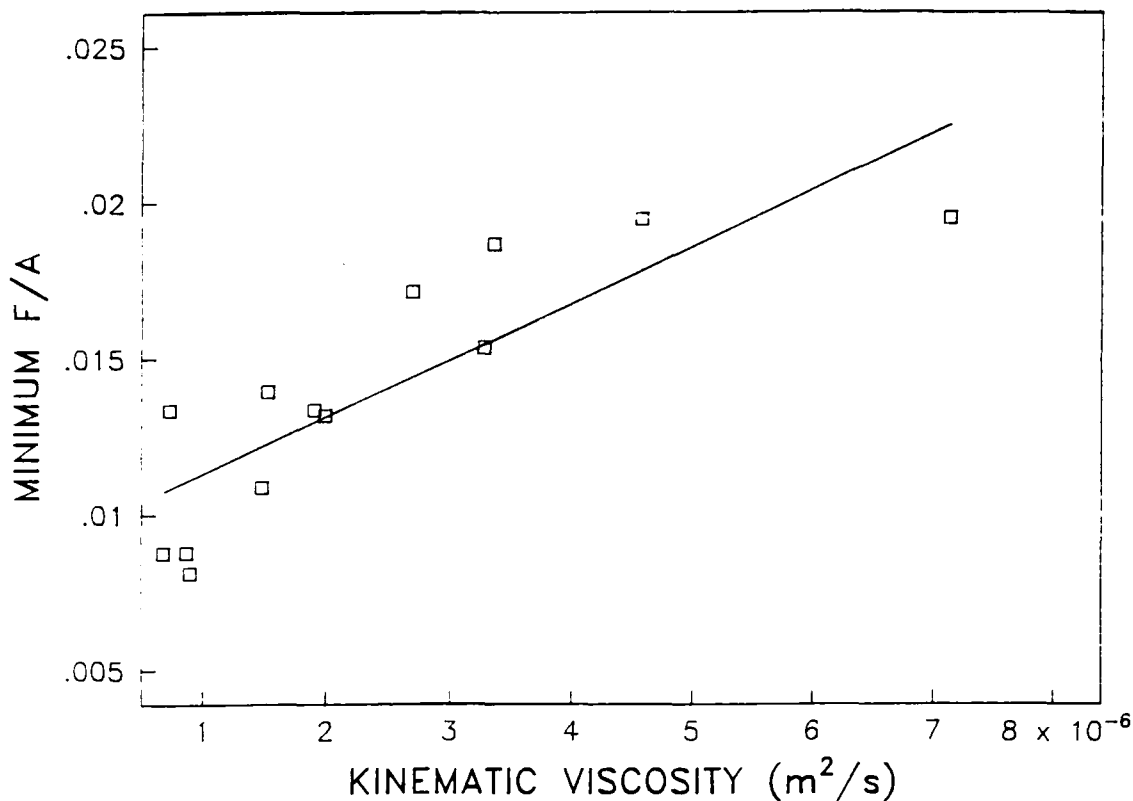
Figure 23. Correlation of minimum fuel/air ratio for ignition with viscosity for the standard T63 atomizer
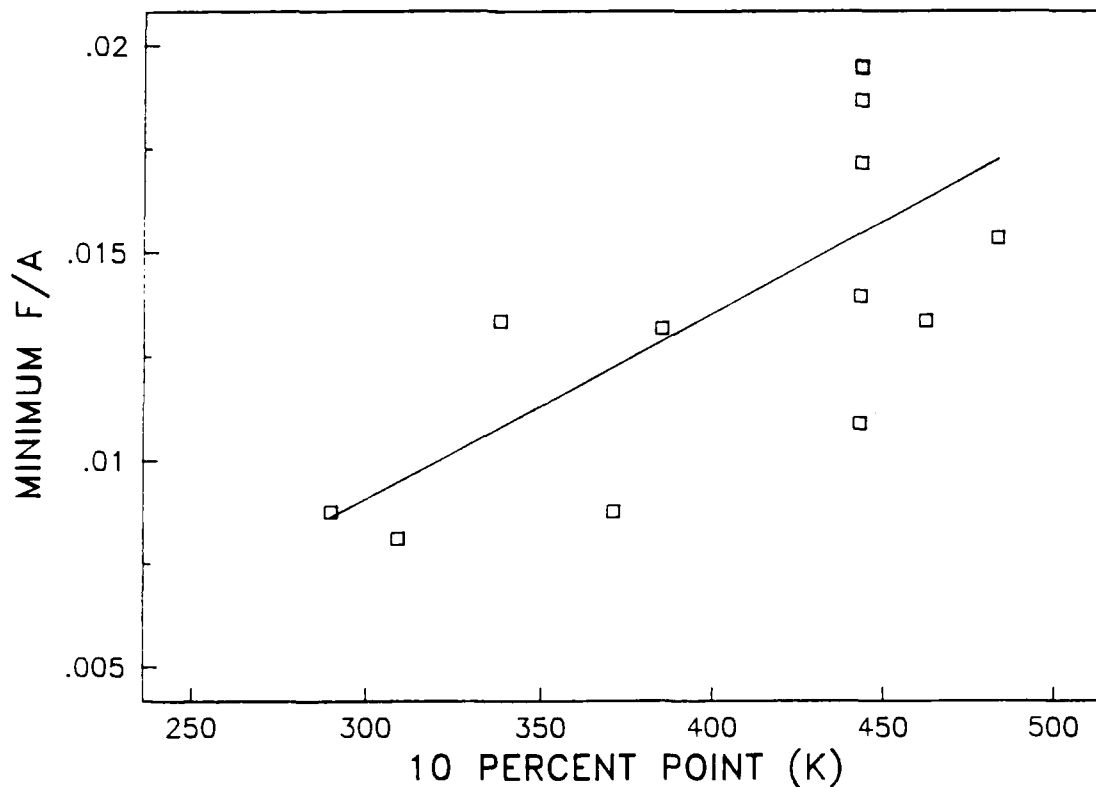
Figure 24. Correlation of minimum fuel/air ratio for ignition with volatility (10 percent pt) for the standard T63 atomizer
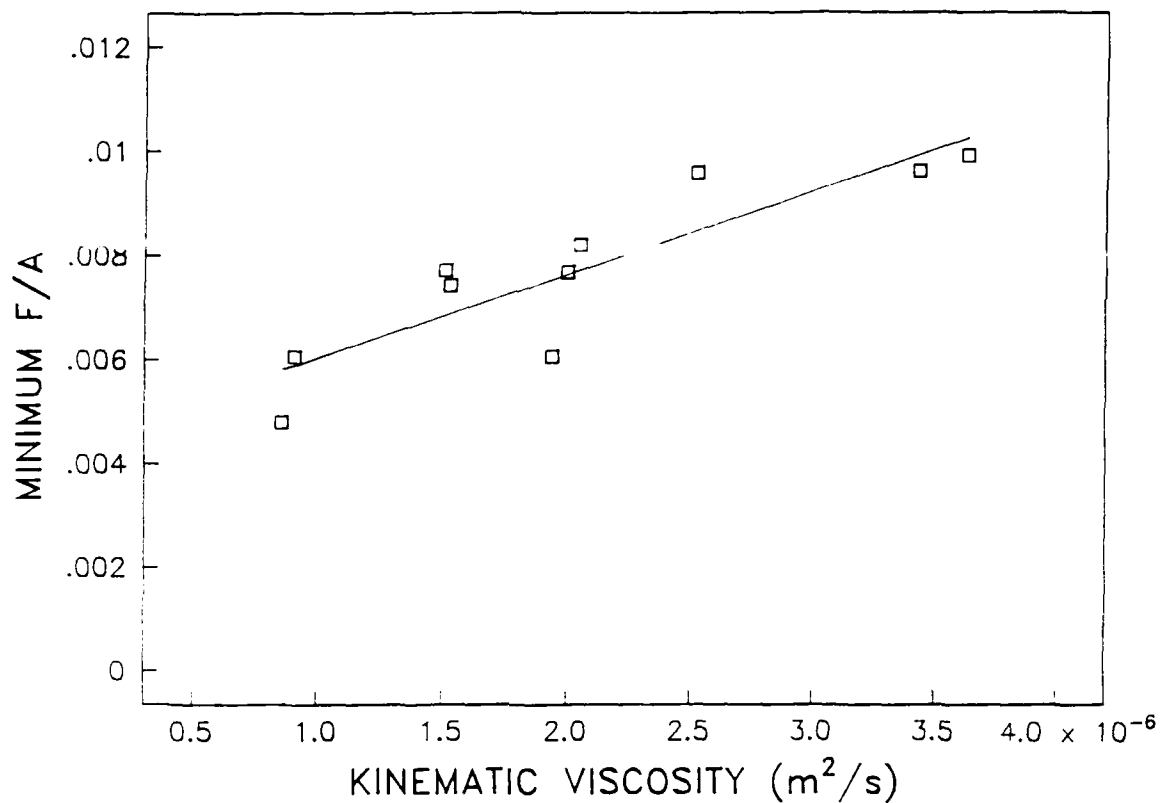
Figure 25. Correlation of minimum fuel/air ratio for ignition with viscosity for the Delavan 4 gal./hr atomizer
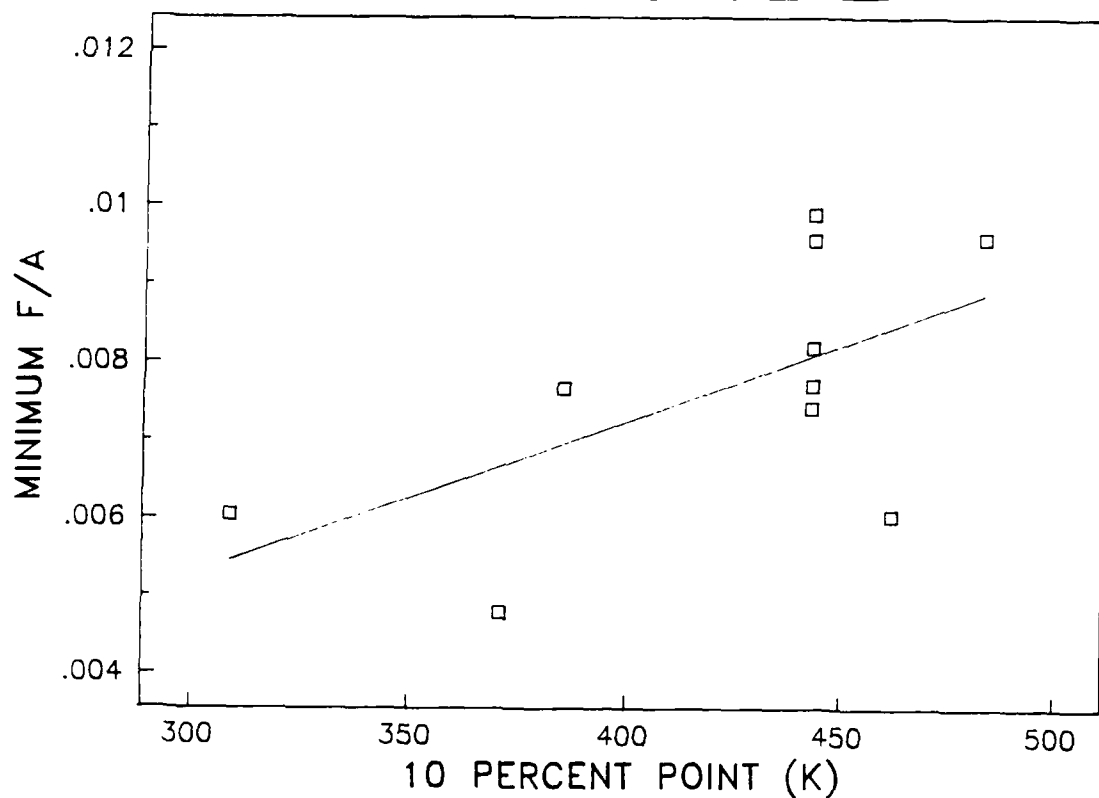
Figure 26. Correlation of minimum fuel/air ratio for ignition with volatility (10 percent pt) for the Delavan 4 gal./hr atomizer
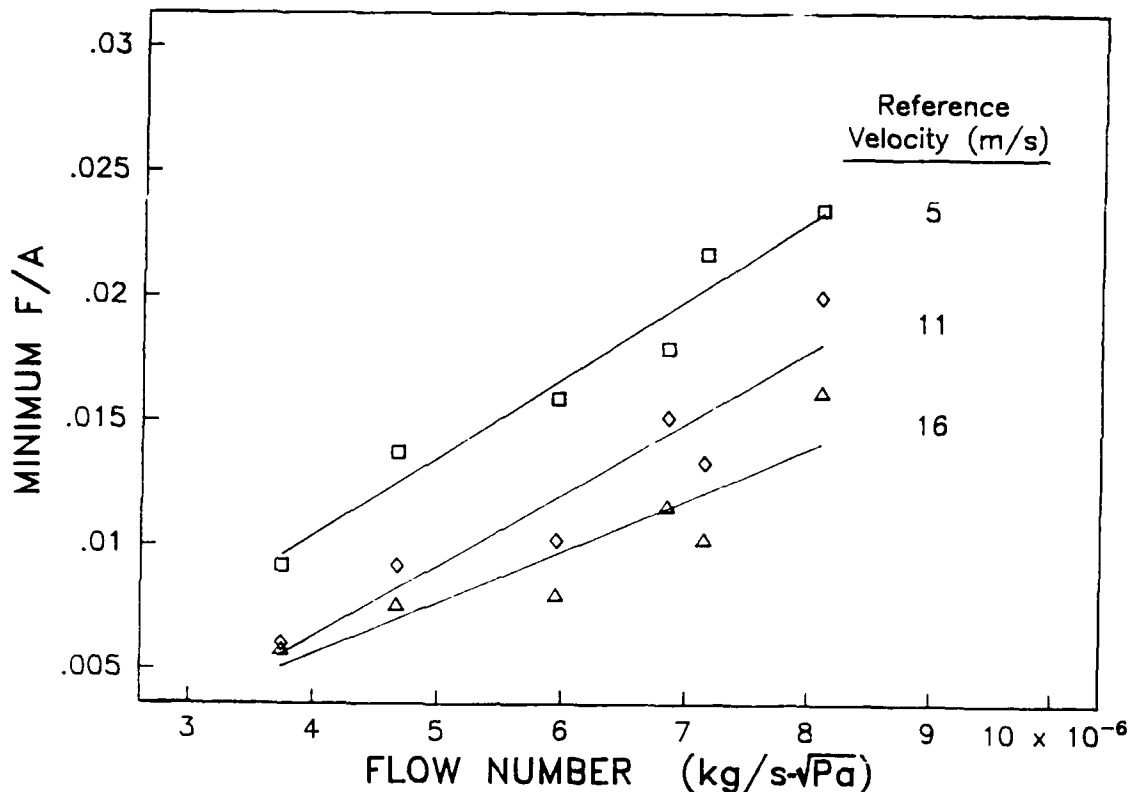
Figure 27. Effect of atomizer flow number on the minimum fuel/air ratio for ignition, JP-5 fuel

with no dependence on atomizer flow number. The fact that the minimum fuel/air ratio for ignition increases with atomizer flow number is a result of the fact that the average drop size of the spray must fall below a critical value for ignition to be successful. For the higher capacity atomizers, this critical SMD is reached at a higher fuel flow rate than for the lower capacity atomizers.

If indeed a critical SMD is the important criteria for ignition, then it should be possible to replot the data in Fig. 27 in terms of SMD at the ignition condition versus atomizer flow number, and the critical SMD should be relatively constant for changing flow number. Fig. 28 is a plot of SMD at the minimum fuel/air ratio ignition condition versus atomizer flow number for the three reference velocities and for JP-5 fuel. (The SMDs were calculated from Eqs. (12) through (14).) Although Fig. 28 illustrates some scatter, the results support the concept of a critical SMD rather than a critical fuel/air ratio for ignition. At the 5 m/s condition, the fuel/air ratio at ignition in Fig. 27 varies by a factor of 2.6, while in Fig. 28 the corresponding SMDs range from 99 to 122, a factor of 1.2. At the 11 m/s and 16 m/s conditions, the respective fuel/air ratio at ignition varied by 3.2 and 2.7; whereas,
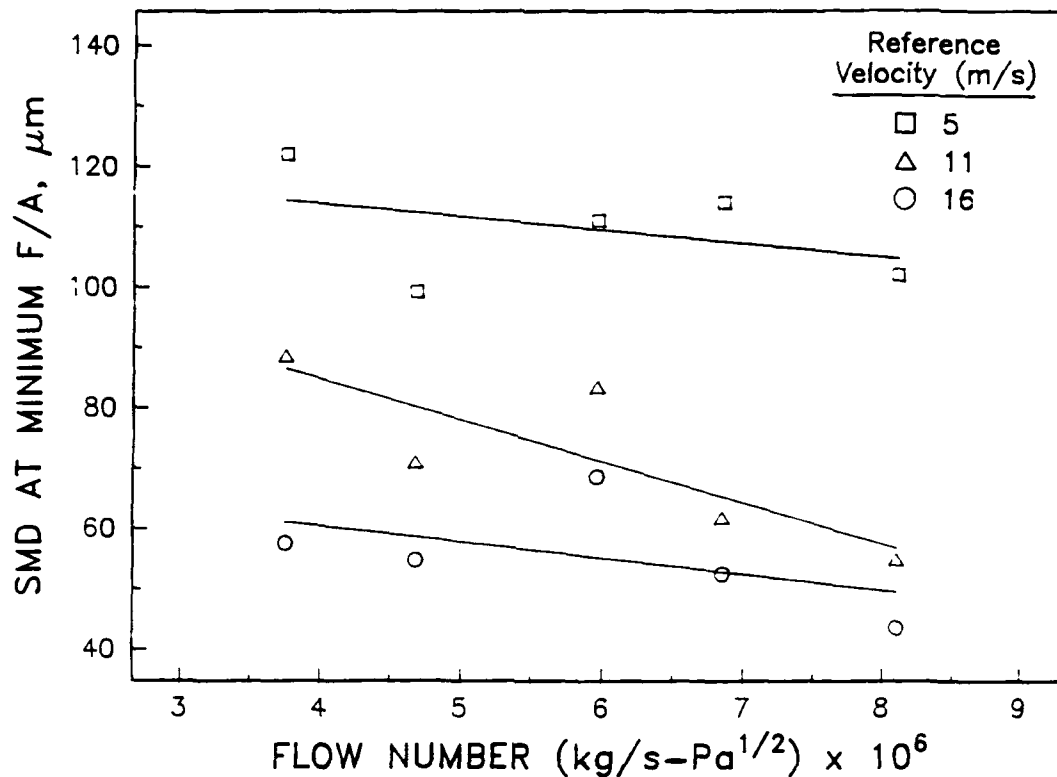
Figure 28. SMD at ignition condition versus atomizer flow number, JP-5 fuel

the corresponding SMDs ranged from 56 to 88, a factor of 1.6, and 43 to 69, a factor of 1.6.

Fig. 28 also shows that the SMDs at the minimum ignition condition decrease with increasing fuel/air ratio. That decrease is explained in terms of turbulent mixing and droplet evaporation that, respectively, govern heat loss and heat generation within the spark ignition kernel. As the reference velocity is raised, the rate of heat loss in the ignition kernel increases due to turbulent mixing. To achieve ignition, the rate of heat generation must increase in proportion with the heat loss. Since droplet evaporation is, for the most part, the process that limits the rate of heat generation, the SMD of the fuel spray must be reduced if the droplet evaporation time is to decrease. This will be presented in more detail later using the characteristic time model approach.

Basically, these observations are of significance to the characteristic time model because they indicate that while ignition strongly depends on SMD, it is essentially

independent of the overall fuel/air ratio. This result is consistent with the measurements made at the spark gap because the fuel/air ratio at the spark gap was found to be essentially independent of the overall fuel/air ratio in the combustor.

In previous combustor studies, the effect of the burner inlet air temperature on ignition has been difficult to discern because of the effect of fuel temperature. In the present study, the fuel temperature effect has been accounted for in the SMD correlations discussed earlier. The fuel temperature has a strong effect on viscosity and surface tension and, hence, also the SMD of the spray. But once the fuel is atomized, droplet temperatures rapidly approach the burner inlet air temperature. In the cold-start ignition process, the burner inlet air temperature has only a small effect on fuel vaporization before droplets reach the igniter; the predominant effect is in how it affects the temperature of the spark kernel. Fuel must vaporize in the spark kernel if it is to ignite. Figs. 29 through 31 show the effect of burner inlet temperature on the calculated SMD at the minimum fuel/air ratio for ignition. Fig. 29 shows data obtained at a reference velocity of 11 m/s with the T63 dual orifice atomizer and Fuels 1 through 8 (see TABLE 1). Figs. 30 and 31 show data obtained at a reference velocity of 11 m/s with the 4- and 8-gal./hr Delavan simplex atomizers and Fuels 1 through 6. The trend lines in the data indicate that as the burner inlet temperature is reduced, smaller SMDs are required to achieve ignition. The more volatile fuels seem to exhibit a stronger effect than the others. In particular, the SMDs calculated for JP-4, and NDF/70 percent gasoline appear to vary more strongly with burner inlet temperature than the less volatile fuels such as JP-8, JP-5, and NDF. However, Fuel 4, NDF/25 percent gasoline, which was blended with a viscosity equal to JP-5 and a volatility similar to JP-4 seems to require an SMD closer in size to that needed by JP-5 and JP-8 to ignite. These observations are speculative because there is considerable scatter in the data. Methanol requires smaller SMDs for ignition because its fuel/air ratio requirement is expected to be about twice that of a hydrocarbon-based fuel. However, based on the minimum fuel/air ratios measured for ignition, methanol ignited at the lowest overall equivalence ratio of all the fuels tested. This low ratio was due to its low viscosity and higher mass flow rate through the atomizer, which resulted in fuel sprays with smaller SMDs.
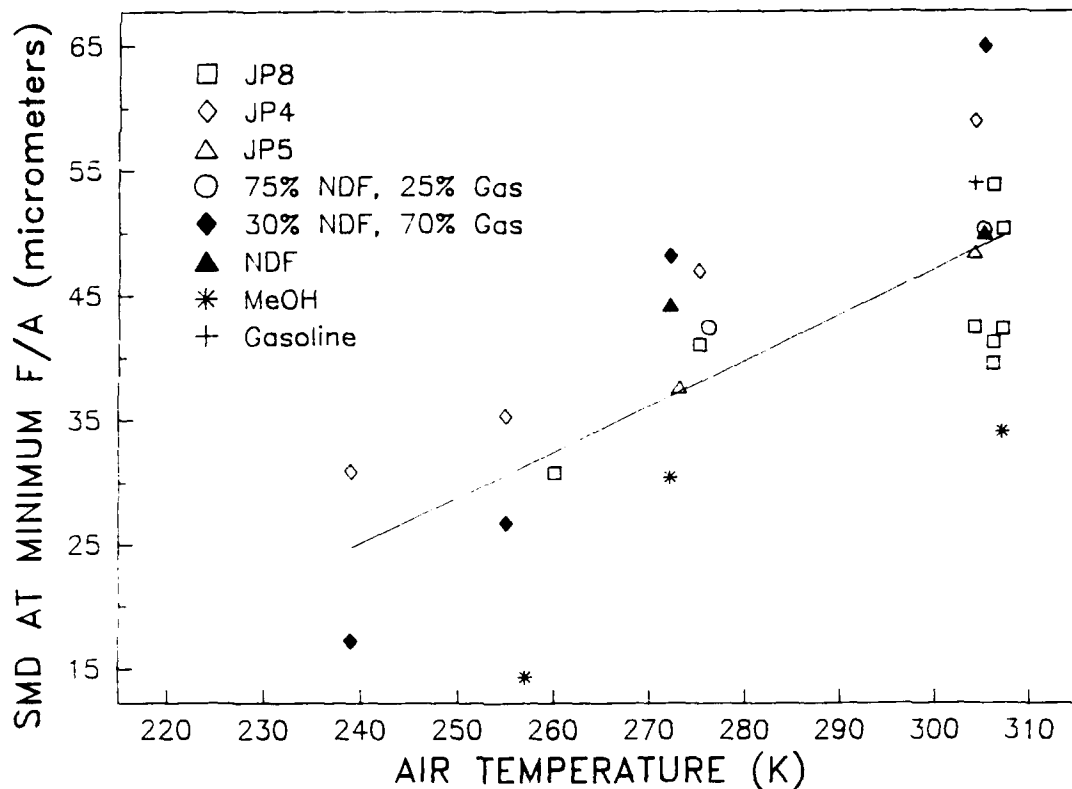
Figure 29. Effect of air temperature and fuel type on SMD required for ignition using standard T63 atomizer
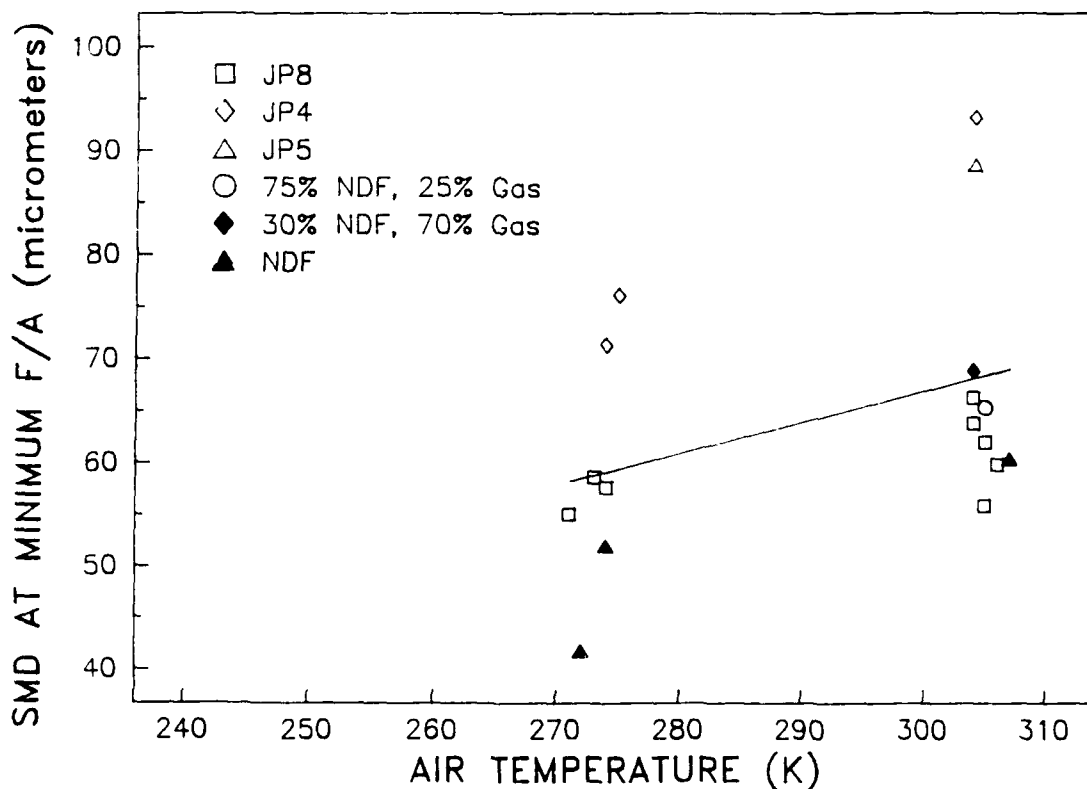
Figure 30. Effect of air temperature and fuel type on SMD required for ignition using the Delavan 4 gal./hr atomizer

42
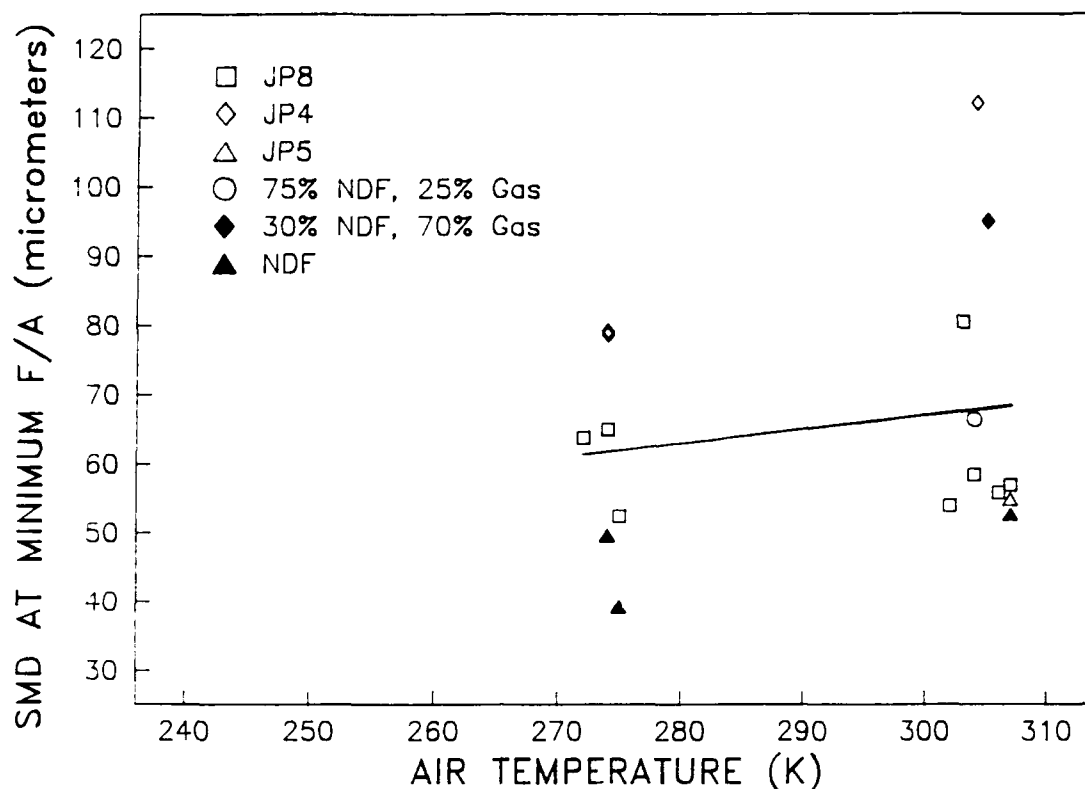
Figure 31. Effect of air temperature and fuel type on SMD required for ignition using the Delavan 8 gal./hr atomizer

Fuel Composition - Ignition of fuel sprays is usually assumed to depend on the physical properties of the fuel, since chemical reaction rates in the ignition kernel are assumed to occur at flame temperatures where they would be relatively fast, and it is the droplet evaporation rate that limits the rate of heat release. Homogeneous gas phase combustion measurements in shock tubes have shown that aromatics such as toluene have significantly longer ignition delays than paraffins.(29) However, these are chemical delays that are expected to be small compared to droplet evaporation times. To examine effects of aromatic content on ignition, high-aromatic Fuels 9 and 10 (see TABLE 1) were blended with viscosities, surface tensions, and 10 percent boil-off temperatures that were essentially the same as those of Fuel 1, JP-8. The aromatics contained in Fuels 9 and 10 were mostly monocyclic; the effect of aromatic type was not investigated. Fig. 32 shows the effect of aromatic content on the minimum fuel/air ratio for ignition. The measurements were made at three reference velocities with a burner inlet and fuel temperature of about 300K. The results in Fig. 32 show that there is a definite increase in the minimum fuel/air ratio as the aromatic content is increased.

43
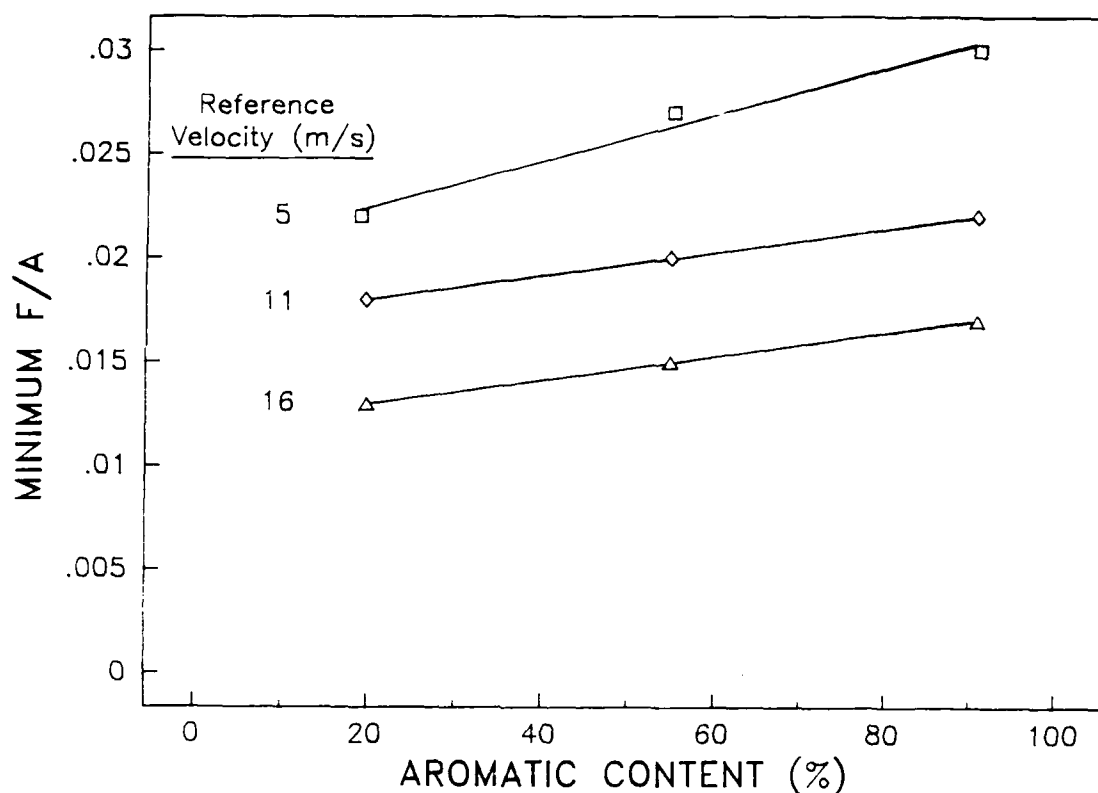
Figure 32. Effect of aromatic content on the minimum fuel/air ratio for ignition

The fact that the minimum fuel/air ratio increases indicates that the SMD of the fuel spray at the ignition limit decreases as the aromatic content increases. This decrease suggests one of two possibilities; either the droplet evaporation rates for Fuels 9 and 10 are much less than that of Fuel 1, or the chemical ignition delay for aromatics is of the same magnitude as the droplet evaporation rate and therefore tends to limit the heat generation rate in the spark ignition kernel. It is not likely that the droplet evaporation rates of Fuels 9 and 10 are different than that of Fuel 1. Fuels 9 and 10 were carefully blended to have the same physical properties as Fuel 1. The only significant fuel-dependent parameter in the droplet evaporation constant, β , is the 10 percent boil-off temperature, which is used to indicate fuel volatility, and that was the same for each of the test Fuels 1, 9, and 10.

Another possibility is that the fuel/air ratio at the lean flammability limit is much higher for aromatics than it is for paraffins. If this were true, the aromatic fuel droplets would need to vaporize to a greater extent before ignition could take place.

44

Comparison of the lean flammability limits of paraffins and aromatics show that there is very little difference in their lean limit fuel/air ratios; e.g., the fuel/air ratios for the lean flammability limits of hexane and benzene are 0.0359 and 0.0388, respectively.

It is well known that reaction rates are very high at flame temperatures. If the gases within the ignition kernel were at flame temperature, the chemical delay would be negligible compared to the droplet evaporation time. However, it is conceivable that chemical delay could be important in the ignition process and especially for fuels with high aromatic content if the temperature in the ignition kernel is relatively low (ca. 1000K). The photographic data (see Fig. 15) support the notion that the temperature in the ignition kernel is well below the stoichiometric flame temperature during the dark zone. As the temperature is reduced, the reaction rates fall rapidly and the chemical delay becomes increasingly important. The effect of temperature on the ignition delay of highly aromatic fuels should be substantially greater than that for normal paraffins because the aromatics have a much higher autoignition temperature.(29) To compensate for the effect of a higher autoignition temperature and greater ignition delay, the droplet evaporation time would have to decrease. This decrease in evaporation time would require a smaller SMD, which corresponds with the higher minimum fuel/air ratio for ignition that was observed experimentally.

Thus, the experiments with the aromatic fuels when combined with the photographic observations of a significant dark period indicate that many of the important reactions leading to ignition must occur at relatively low temperatures (compared with flame temperatures) where reactions rates are slower and autoignition temperatures are more significant. Under these relatively lower temperature conditions, reaction rates may be of the same magnitude as evaporation rates.

E. Characteristic Time Model Analysis

The characteristic times for turbulent mixing, droplet evaporation, and oxidation chemistry were calculated with a computer code obtained from Mellor (15) at Drexel University. Before the code was applied to the ignition data obtained in this study, several changes were made. The changes were made (1) to simplify data

acquisition and make the code more versatile, and (2) incorporate the new information on fuel/air ratio and gas velocity at the spark gap.

One rather time-consuming aspect of preparing the ignition data for the model was the calculation of flame temperatures. The flame temperature calculations were formerly performed with a SwRI code similar to the NASA code.(30) The calculated flame temperatures were used as input for the characteristic time model code. The flame temperature was usually calculated at the stoichiometric adiabatic condition, but if the temperatures were desired at a different equivalence ratio, the calculations had to be repeated and the new temperatures entered into the CTM data file. The alternative to this very time-consuming process was to include an algorithm for calculating flame temperature in the code. Two such algorithms were found in the literature.(31, 32) The algorithm developed by Gülder (31) for specifically calculating the flame temperatures of jet fuels was used in the CTM code. Since the flame temperature could be calculated at any equivalence ratio by the algorithm in the code, it seemed consistent to also include correlations for other parameters such as the thermal conductivity of air and the heat capacities of both fuel and air. In the original code, the calculations were restricted to stoichiometric flame temperatures so only average values of parameters such as heat capacity and thermal conductivity were used.

The SMDs of the fuel sprays in the combustor were calculated using Eqs. (12) through (14) given earlier in this report. The fuel properties used in the calculations were measured at a single reference temperature. The following expressions were used to interpolate the fuel density, surface tension, and viscosity at the test temperature. Average values of the gradients and the exponent, a, were used in the calculations; these parameters were essentially the same for all the test fuels.

Fuel density:

$$\rho_T = \rho_{T_o} + \frac{\partial \rho}{\partial T}(T_o - T) \tag{15}$$

Surface tension:

$$\sigma_T = \sigma_{T_o} + \frac{\partial \sigma}{\partial T}(T_o - T) \tag{16}$$

Viscosity:

$$\nu = \left[\nu_{T_o} + 0.7 \right]^{(T_o/T)^a} -0.7 \tag{17}$$

where

T_o	= reference temperature
ρ_{T_o}, σ_{T_o}, and ν_{T_o}	= fuel property values at T_o
a	= the viscosity temperature gradient

In view of the measurements of fuel/air ratio and gas velocity at the spark gap, the equivalence ratio dependence of the characteristic times was deleted from the code, and the reference velocity was replaced by the correlation for V_{sg} given by Eq. (11). Since the velocity at the spark gap is about an order of magnitude smaller than the reference velocity, the Reynolds number effect on the droplet evaporation rate in Eq. (5) was changed from $0.185Re^{0.6}$ to $1 + 0.3Re^{0.5} Pr^{0.33}$ as suggested by Ranz and Marshall.[21]

Flame temperature is an important parameter in the model because it is assumed to be the temperature within the spark kernel where the heat from the spark and that generated by chemical reaction is being dissipated by turbulent mixing and fuel evaporation. The actual temperature within the spark kernel is unknown, and probably varies significantly throughout the ignition process. Based on the high-speed photographic evidence and the tests with aromatic fuels, the kernel temperature during the dark period appears to be substantially less than the stoichiometric flame temperature.

If ignition is possible only after the fuel vapor/air ratio in the spark kernel reaches the lean limit, it is the flame temperature at the lean limit that should be used instead of the stoichiometric flame temperature. In accordance with this view of the ignition process, the flame temperatures used in calculating the characteristic times were those calculated at the lean limit equivalence ratio ($\phi = 0.5$).

The results of the characteristic time model calculations on the ignition data obtained on each of the six atomizers examined in this study are shown in Figs. 33 through 38. Each figure shows a correlation of the turbulent mixing time with the

47
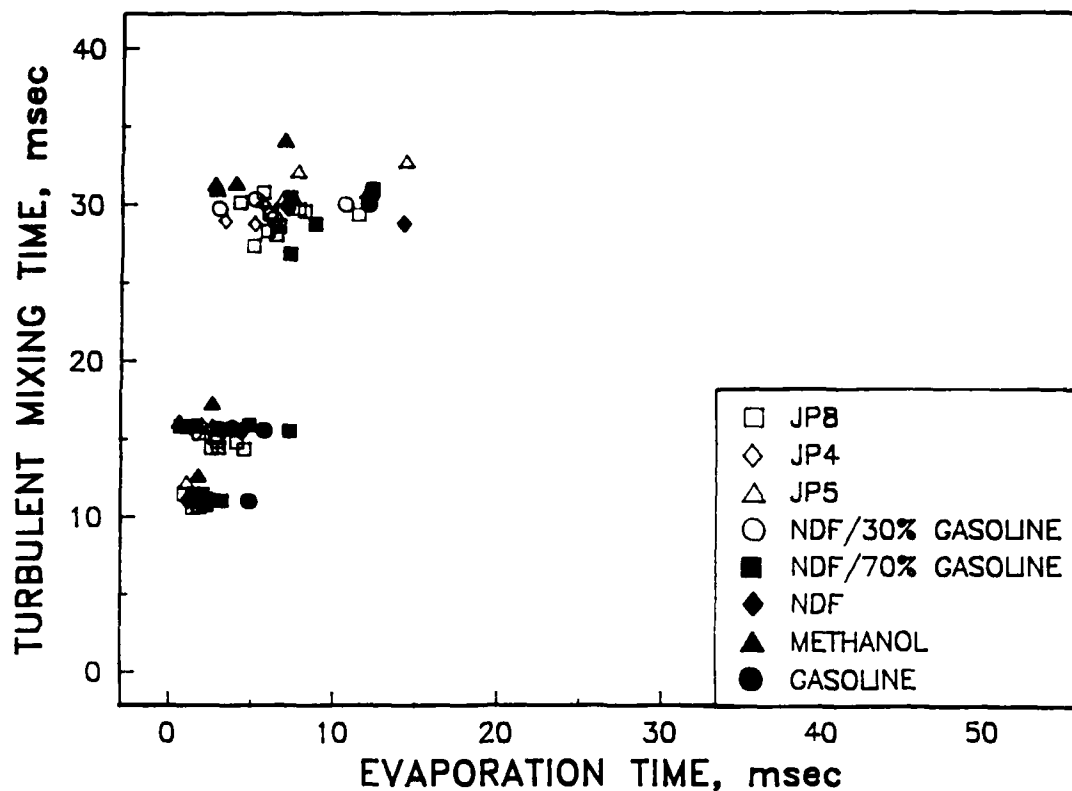
Figure 33. Correlation of turbulent mixing time with drop evaporation time for ignition experiments conducted with the standard T63 atomizer
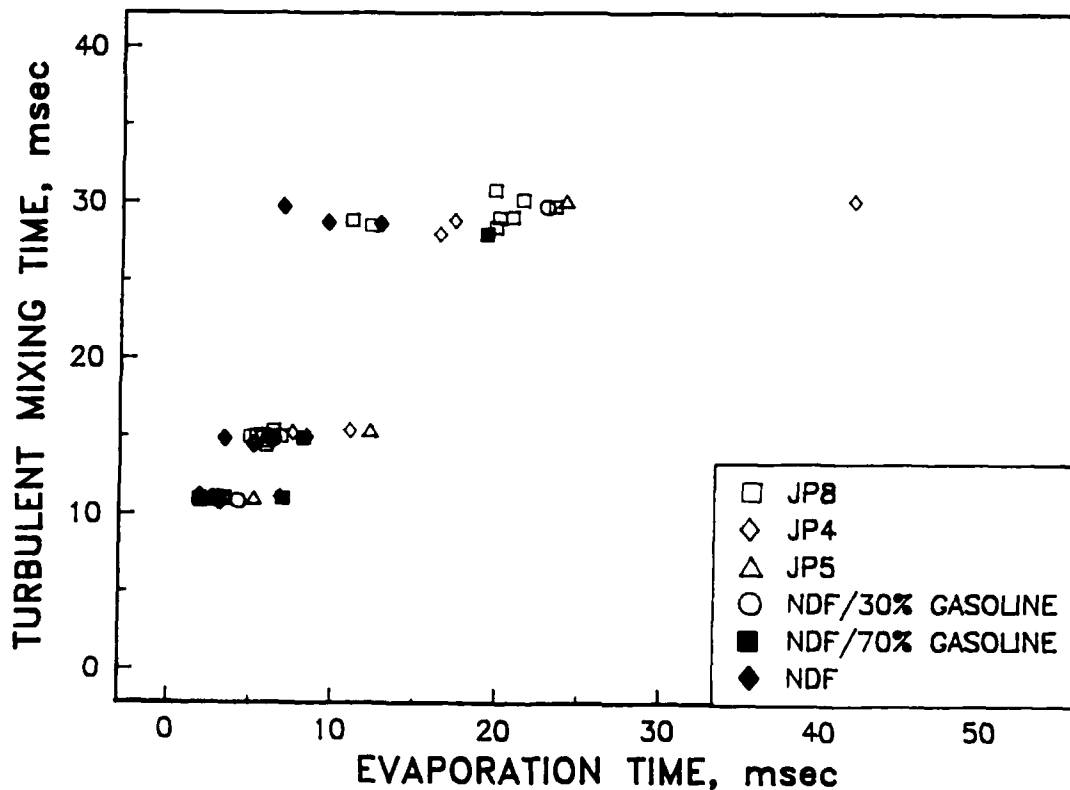
Figure 34. Correlation of turbulent mixing time with drop evaporation time for ignition experiments conducted with the Delavan 4 gal./hr atomizer

Figure 35. Correlation of turbulent mixing time with drop evaporation time for ignition experiments conducted with the Delavan 5 gal./hr atomizer

Figure 36. Correlation of turbulent mixing time with drop evaporation time for ignition experiments conducted with the Delavan 6 gal./hr atomizer

Figure 37. Correlation of turbulent mixing time with drop evaporation time
for ignition experiments conducted with the Delavan 7 gal./hr atomizer

Figure 38. Correlation of turbulent mixing time with drop evaporation time
for ignition experiments conduct d with the Delavan 8 gal./hr atomizer

droplet evaporation time for ignition data from one atomizer. The chemical kinetic time is not included in these correlations because it was assumed to be small compared to the droplet evaporation time; heat generation was assumed limited entirely by the rate of fuel vaporization. Note that this simplification is based on the assumption that the temperature in the kernel is the lean limit flame temperature, i.e., about 1600K. Ignition could occur at temperatures as low as the autoignition temperature. Methane is known to have one of the highest autoignition temperatures (ca. 905K), which is more than 200K above the autoignition temperatures of jet fuels. If the temperature within the ignition kernel were to be as low as 1000K, the chemical kinetic time could well become significant. Clearly, the temperature in the kernel during the dark period is a measurement that should be considered before more serious attempts are made to model the ignition process.

The correlations shown in Figs. 33 to 38 have some similarities and some distinct differences. Note that the computed evaporation times and turbulent mixing times are similar in magnitude. Least square fitted lines of the data present in each figure are not shown because they are strongly affected by lateral scatter in the low reference velocity data, i.e., data with turbulent mixing times of about 30 msec, which tend to bias the least squares fit. Fitting a least squares straight line results in an unreasonably low slope and a high intercept. However, if one imagines a straight line through the data, it becomes evident that the curves intercept the turbulent mixing time axis in the range of approximately 2 to 7 msec, and the slopes of the curves, for data from each atomizer, vary significantly. Ideally, the intercepts should equal zero and the slopes should be the same. It is apparent that the slope and intercept are affected by the atomizer and the fuel type. The evaporation times are much smaller and the slope is much greater for the data from the standard T63 atomizer than from the 7 gal./hr Delavan atomizer. Both of these atomizers have nearly identical flow numbers, but different cone angles. The minimum fuel/air ratios required for ignition of the standard T63 atomizer sprays were greater than those required of sprays produced with the 7 gal./hr Delavan atomizer. However, it is important to note that it is the SMD of the spray that is used in calculating the evaporation time, not the droplet size in a particular sector of the spray volume. By simply changing atomizer parameters such as the cone angle and the droplet penetration depth, it is possible to cause significant changes in the droplet-size distribution that reaches the spark gap. This change in cone angle

51

and penetration may well explain the differences in the slopes of the imaginary curves through the data in Figs. 33 to 38.

The lateral scatter in the correlations, which is the greatest at the low reference velocities, appears to be fuel related. This fuel related scatter is most evident in the correlations of the data from the Delavan simplex atomizers (Figs. 34 to 38). It is apparent that the calculated droplet evaporation times for the more volatile fuels are much longer than those for the less volatile fuels. JP-4 and particularly NDF/70 percent gasoline had longer calculated evaporation times than the less volatile JP-5, JP-8, and NDF fuels. The longer evaporation times indicate that JP-4 and NDF/70 percent gasoline were able to ignite with larger drop sizes than the less volatile fuels.

Note also that one can imagine relatively straight lines passing through individual fuel data points; such correlations look more favorable when the data points for each fuel are considered separately. Similar trends are found in the T63 atomizer data. Fig. 39 shows an expanded version of the points plotted in Fig. 33.

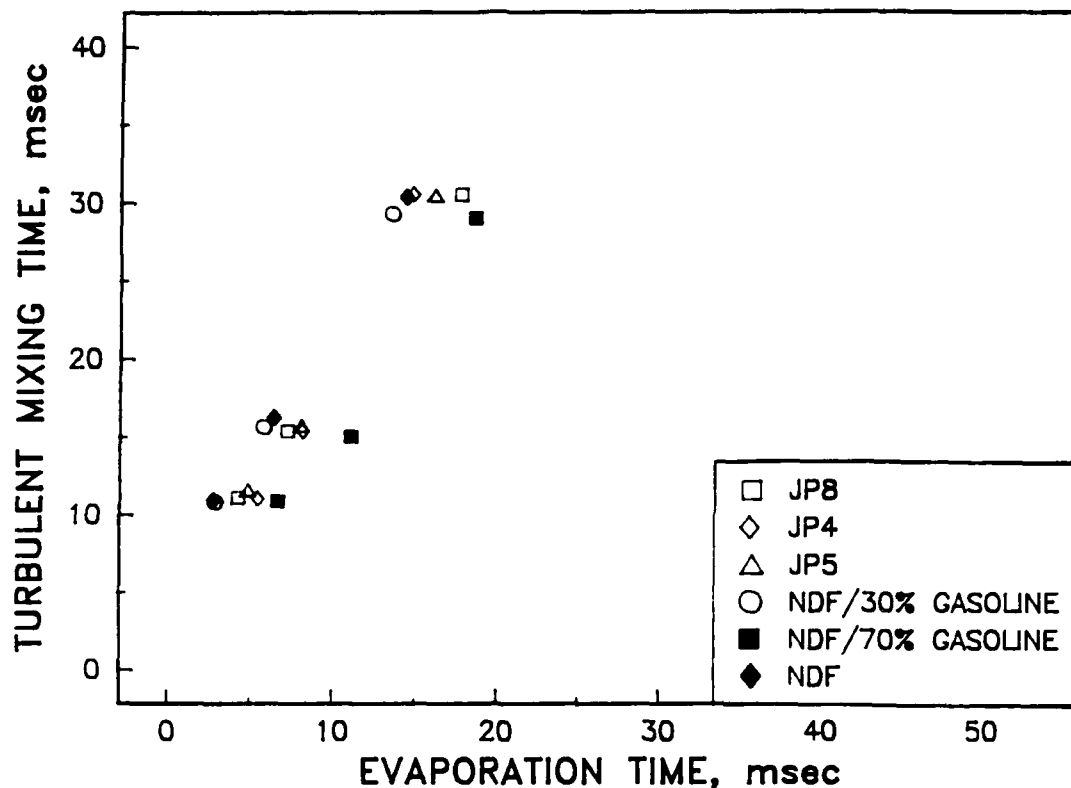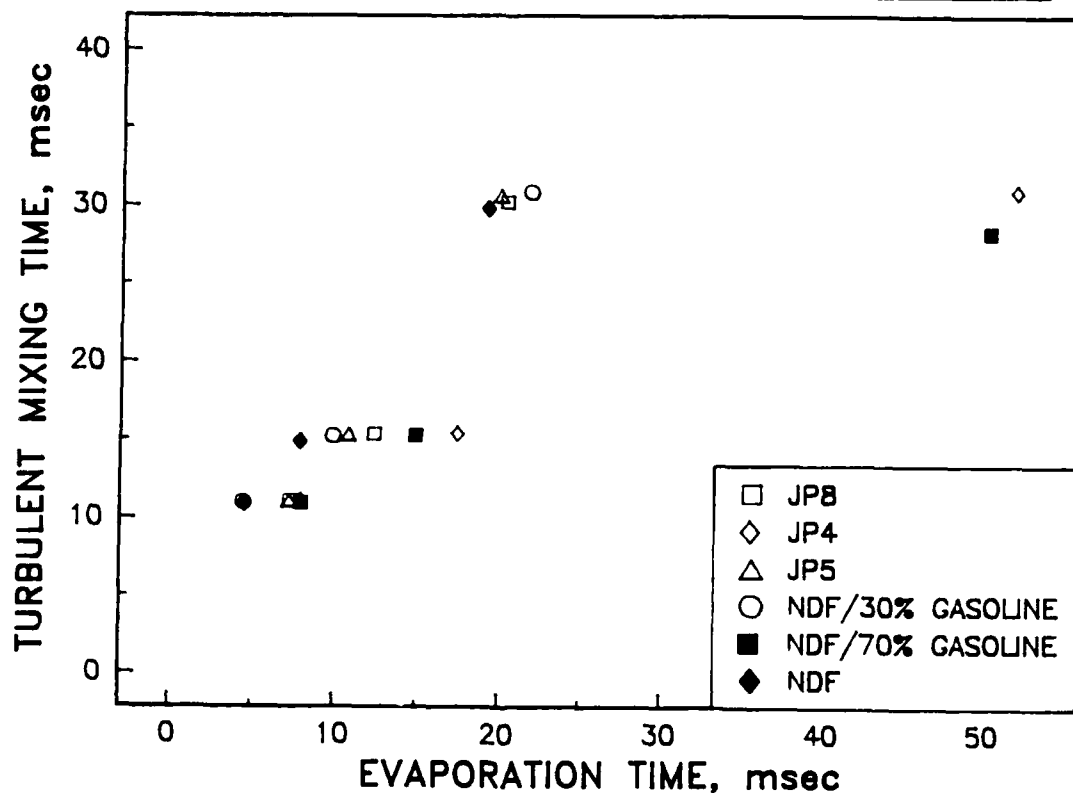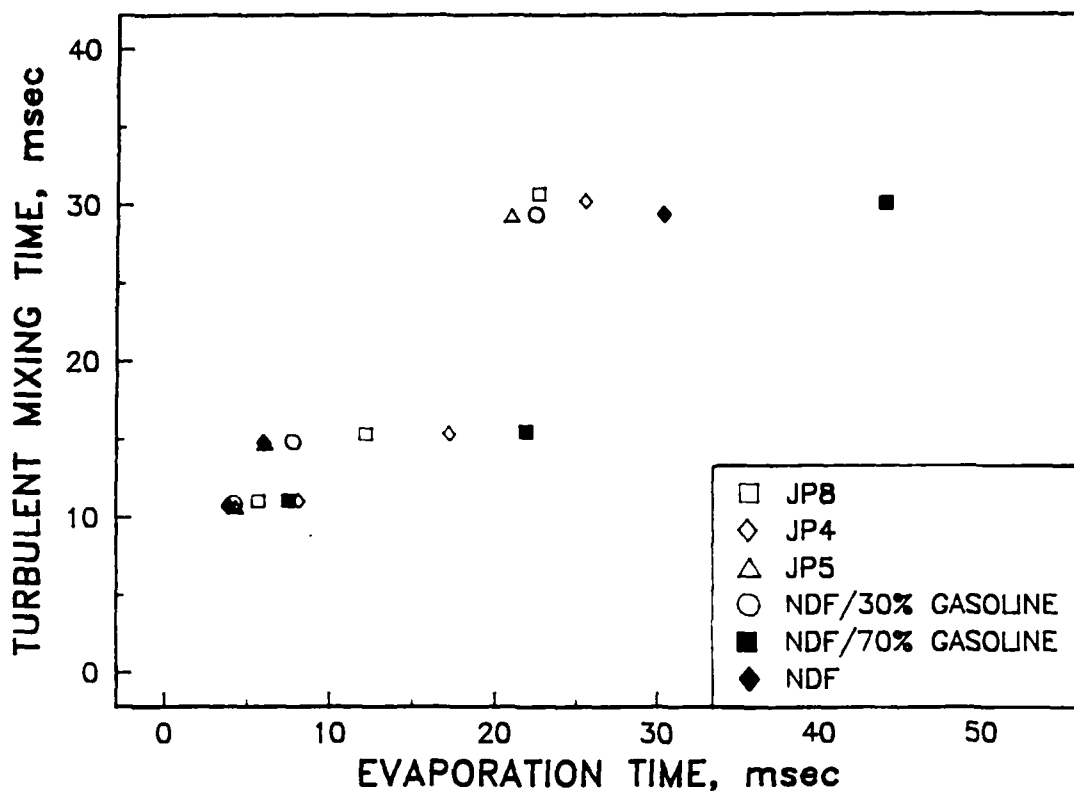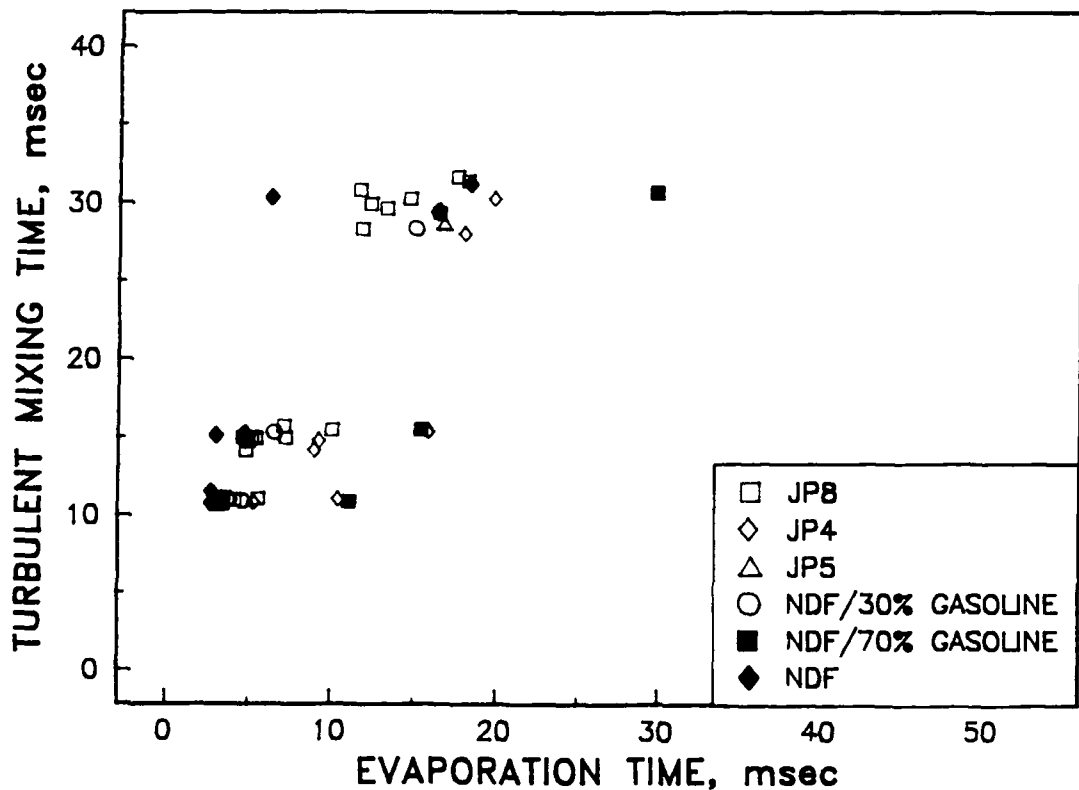Figure 39. Correlation of turbulent mixing time with drop evaporation time for ignition experiments conducted with the standard T63 atomizer (Same as Fig. 33 except for the expanded scale)

Despite the greater degree of scatter and confusion in this plot, the fuel trends relating to volatility are still evident. Fuels 5 and 8, containing high concentrations of gasoline, tend to have longer calculated evaporation times, suggesting that the model does not properly account for fuel volatility effects.

In Figs. 35 to 37, the ignition data on the respective 5-, 6-, and 7-gallon/hour atomizers were measured at ambient conditions, so the lateral scatter in evaporation times for the various fuels is independent of temperature. In Fig. 35, the scatter in the evaporation times is relatively small. The scatter in Figs. 36 and 37 would also be relatively small except for the JP-4 and NDF/70 percent gasoline data points. These results suggest that the lateral scatter is attributable to the fuel volatility, i.e., fuel properties that affect the droplet evaporation constant.

In the characteristic time model, the effect of boiling point on the transfer number is very dependent on the temperature in the ignition kernel. In previous studies (12-15), this temperature has been assumed to be the stoichiometric adiabatic flame temperature. The flame temperature (ca. 2300K) is such a large number in comparison to the boiling point that the difference in the numerator of the transfer number (Eq. 6) is not dramatically different for all fuels ranging diversely in volatility. Even when the temperature is lowered to the flame temperature at the lean limit (ca. 1600K), the effect of boiling point on the evaporation time is not great. The temperature effect is illustrated in Fig. 40 where the droplet evaporation time is plotted versus the boiling points of C5 to C10 alkanes. A significant variation in the droplet evaporation time with boiling point is not observed until the temperature in the ignition kernel is closer to 1000K.

In view of the fact that the autoignition temperatures are well below 900K, it is not unreasonable to believe that the actual ignition temperature in the kernel is on the order of 1000K. The measurements of the high aromatic Fuels 9 and 10 showed that higher minimum fuel/air ratios and, thus, smaller SMDs were required to achieve ignition than for JP-8. Fig. 41 shows a plot of the turbulent mixing time versus the droplet evaporation time for Fuels 1, JP-8; Fuel 9, JP-8/50 percent aromatics; and Fuel 10, heavy aromatics. It is evident in this figure that much shorter droplet evaporation times are required for the ignition of highly aromatic fuels, and it is
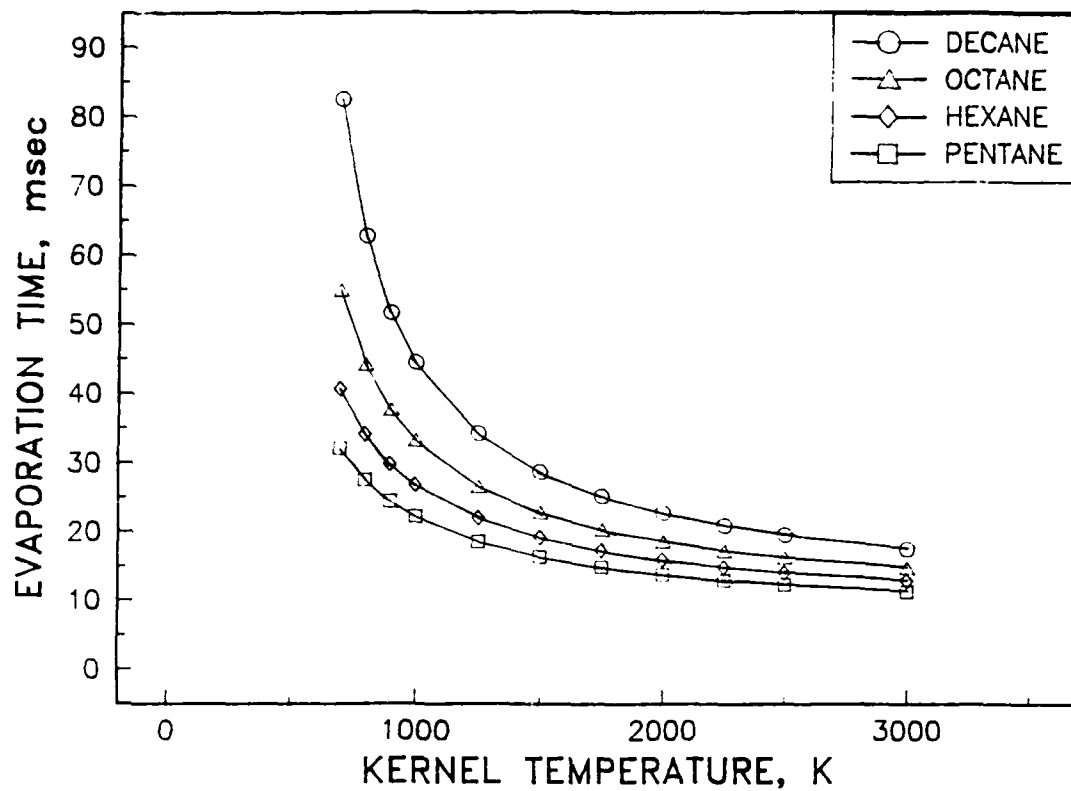
Figure 40. Effect of kernel temperature and fuel type on evaporation time for 100-micrometer droplets of normal alkanes
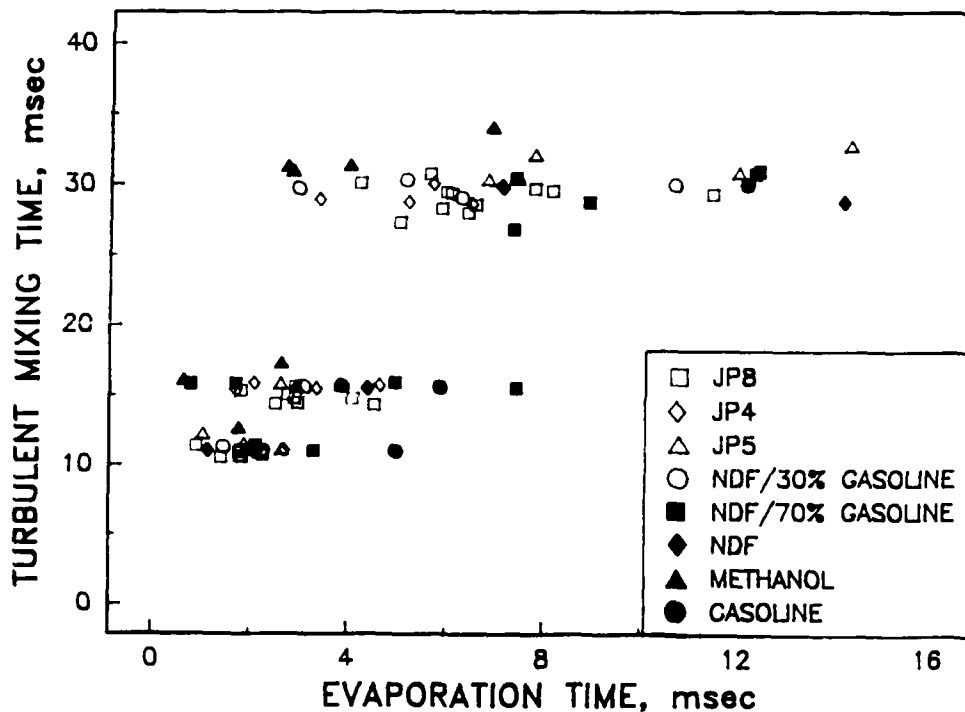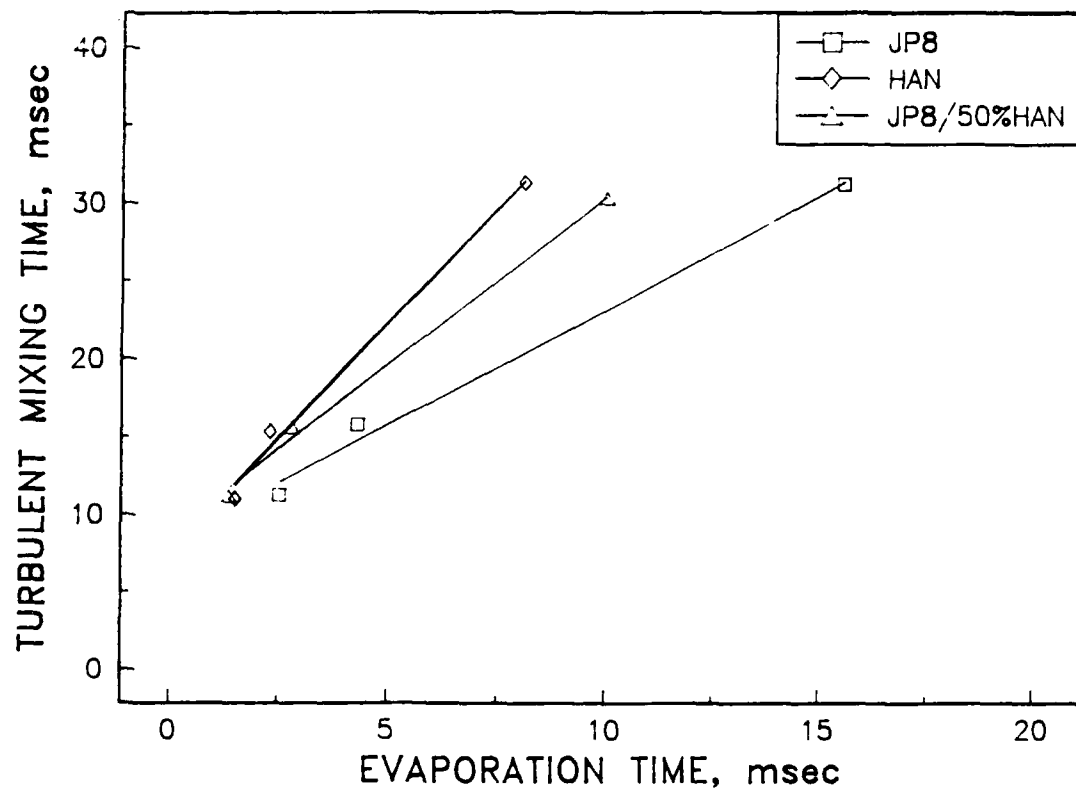

Figure 41. Correlation of turbulent mixing time with drop evaporation time for ignition experiments conducted with fuels of varying aromatic content using the standard T63 atomizer

interesting to note that aromatics have much higher autoignition temperatures than paraffins.(29)

If the temperature in the ignition kernel is close to the stoichiometric flame temperature, there would be little or no effect of autoignition temperature on the ignition process because the chemical kinetic time would be very short and the evaporation time would be the only factor limiting the rate of heat generation. However, if the temperature in the kernel is low (ca. 1000K), the chemical time could well become comparable with the evaporation time, and it might then be expected that the ignition delay time would increase as the aromatic content of the fuel is raised. However, the high-speed photographs of the ignition of Fuel 10 showed that its ignition delay or dark period was about the same as that observed with JP-8. In view of these facts, it seems that the chemical time for Fuels 9 and 10 were greater than that for Fuel 1, but to prevent a further increase in the ignition delay, the droplet evaporation time had to decrease. This is why higher fuel flows were required for the aromatic fuels, i.e., to decrease the SMD of the fuel spray.

It may be concluded from the arguments given above that ignition and flame propagation must occur within a certain period of time; otherwise, the temperature within the kernel will fall below a threshold for ignition. Thus, the combined rates of chemical reaction and droplet evaporation must exceed the rate of cooling of the ignition kernel. This model is illustrated schematically in Fig. 42, which shows that for a successful ignition event the drop evaporation and precombustion reactions must be completed before the ignition kernel temperature drops below the autoignition temperature of the fuel. As the velocity and/or turbulence levels increase, the kernel temperature decreases more rapidly, making ignition more difficult. Note that the autoignition temperature of aromatics is higher than paraffins, corresponding to the experimental observation that they are more difficult to ignite.

It should be noted that the main heat source for the ignition process is the energy of the spark. The precombustion reactions responsible for producing the free radical precursors necessary for propagation of the combustion process are, for the most part, thermoneutral and thus contribute very little enthalpy to the gases within the spark kernel. Several studies (33) in a turbulent flow reactor have shown that
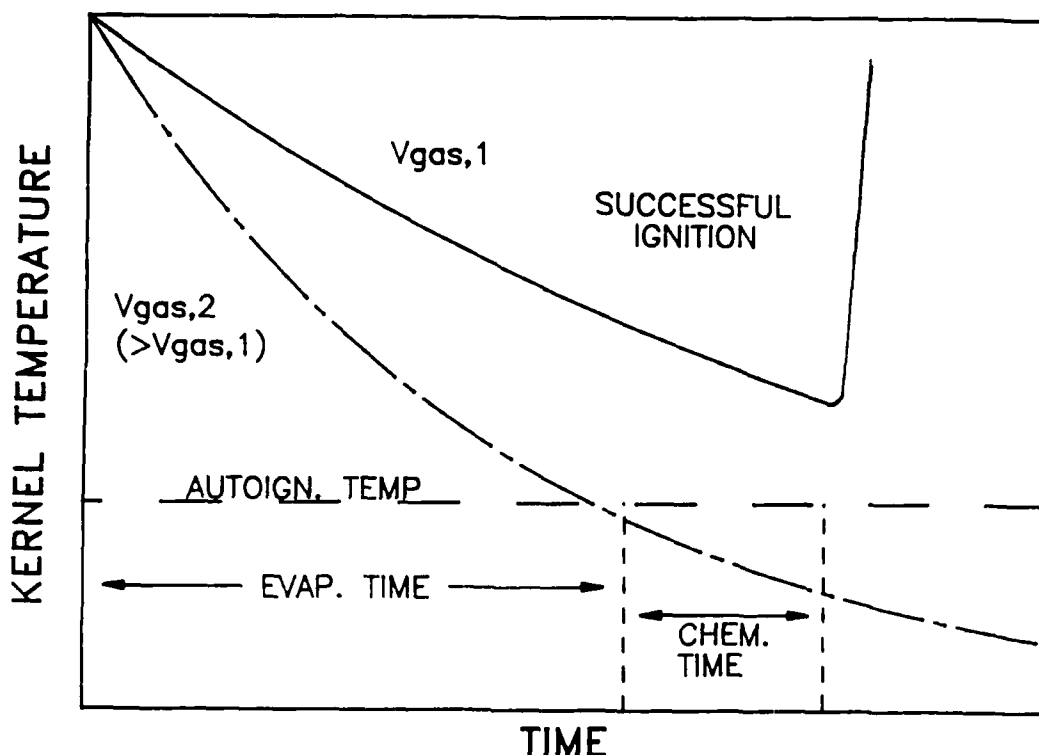
Figure 42. <u>Schematic representation of new characteristic time model showing that</u>
<u>for a successful ignition the drop evaporation and precombustion reactions must</u>
<u>be completed before the ignition kernel temperature drops below the</u>
<u>autoignition temperature</u>

considerable oxidative decomposition of the fuel and partial oxidation to carbon monoxide and water occur before there is a substantial rise in the temperature.

This interpretation of the results suggests a modified version of the characteristic time model. In the original CT model the ignition limit is defined as the condition where the heat loss term, T_{sl}, is balanced by the heat generation terms, T_{hc} and T_{eb}. In the new model, T_{sl} is the time it takes for the ignition kernel to cool to the autoignition temperature of the fuel. In the period, T_{sl}, there must be sufficient droplet evaporation and precombustion reaction to achieve flame propagation. Basically, the relationship between the characteristic times is the same,

$$T_{sl} = T_{hc} + T_{eb}, \tag{18}$$

for the ignition limit condition, but the concept is different in that Eq. 18 is a balance of rate processes rather than heat loss and heat generation terms.

V. CONCLUSIONS

Extensive experiments were carried out in a T63 gas turbine combustor to verify assumptions made in the characteristic time model for correlating ignition data. Measurements of gas velocity and fuel/air ratio were made at the spark gap. High-speed photographs of the ignition process in the combustor were taken, and approximate ignition delay times were measured. Cold-start ignition data were obtained at temperatures ranging from 25° to -34°C on ten fuels over a wide range of conditions. Six atomizers of varying flow capacities were used in the combustor tests. SMD measurements were made on each of the atomizers, and correlations of SMD with the flow conditions and fuel properties were developed. The following conclusions were drawn from the results.

Ignition depended more strongly on achieving a critical average drop size (SMD) than on reaching the lean-limit fuel/air ratio. The fuel/air ratio measured at the spark gap at the minimum ignition condition was significantly in excess of the lean-limit in all cases.

Fuel viscosity, which determines atomization characteristics, was more important than volatility in the ignition process. The importance of viscosity was particularly true for fuels such as JP-5, JP-8, and less volatile fuels. Volatility was significant for JP-4 and gasoline-type fuels. Previous characteristic time model correlations for ignition underestimate the effect of volatility by using too large a reference temperature in calculating the transfer number for drop evaporation. Lowering that temperature even to the adiabatic lean-limit flame temperature (ca. 1600K) still leads to an underestimate of the volatility effect. A reference temperature approaching the autoignition temperature may be more appropriate.

The degradation of ignition performance at low temperature appeared to depend more on the effect of fuel viscosity than on the reduction in the air temperature. However, further tests independently varying the fuel and air temperatures would be required to verify this observation. This observation has the important practical implication that heating the fuel or using a lower viscosity fuel would be a much more efficient way to improve low-temperature ignition than heating the inlet air for combustors using pressure-swirl atomizers for ignition.

High-speed photography showed significant delays (up to 12 ms) from the time the spark formed the ignition kernel to the onset of visible flame radiation. This observation, combined with results showing extended ignition delay periods for fuels with high aromatic content indicated that many of the critical steps for ignition occur at temperatures much lower than adiabatic stoichiometric flame temperatures. These results form the basis for a new characteristic time model that is not based on a balance of heat loss and heat gain at the adiabatic stoichiometric flame temperature, but rather a heat loss from the initial spark until ignition occurs or the temperature drops below the autoignition temperature. A complete evaluation of this new model was beyond the scope of this program.

Finally, two assumptions regarding the characteristic time model were confirmed. First, the air velocity at the spark gap is proportional to the reference velocity through the combustor. Second, the fuel/air ratio at the spark gap was relatively constant independent of overall fuel/air ratio, and was significantly richer than the lean-limit for combustion at the minimum ignition condition.

Correlations of the turbulent mixing time with the droplet evaporation time were reasonably good for individual fuels, but when all the fuels were considered together, there was substantial scatter in the data. Fuels of high volatility exhibited significant deviations from the other fuels, indicating that the effect of fuel boiling point was not given sufficient weight in the characteristic time model. The use of lower effective ignition temperatures as discussed for the new characteristic time model might address these discrepancies.

VI. RECOMMENDATIONS

This work has provided new insight into the ignition process for gas-turbine combustors using pressure-swirl atomizers during the ignition process. In particular, through independent variation of fuel/air ratio and average fuel drop size, it was demonstrated that a critical drop size was more important than a critical fuel/air ratio for ignition. Also a new philosophy for the characteristic time model was developed in which the ignition kernel continuously drops in temperature until self-sustained combustion occurs or the temperature drops below the autoignition temperature.

However, certain questions and concerns remain about using the characteristic time model for predicting ignition performance. Five areas of concern may be listed. First, the effects of fuel volatility are not completely accounted for, especially for highly volatile fuels such as JP-4. Second, although fuel drop size has been shown to be critical to the ignition process, the effect of spray cone angle and airflow on getting drops to the igniter is not well understood. Third, the applicability of the characteristic time model to ignition using a pure airblast atomizer has not been demonstrated. Fourth, it appears that fuel temperature is more important than air temperature in low-temperature ignition, but this possibility should be verified directly. The final area of concern is that little seems to be known about the temperature history of the ignition kernel during the dark period following the initial spark discharge.

The first question concerning volatility effects could be most easily addressed by conducting ignition tests with pure compounds. Pure compounds have unquestionable boiling points and very well-known chemical and physical properties such as heat of vaporization, specific heat, viscosity, and surface tension. Also, actual rate expressions are available for calculating the chemical delay time as a function of temperature. The fuel matrix should consist of normal alkanes to investigate the effects of physical properties on ignition, and some aromatics to be compared with the alkanes to determine the effect of chemical properties. A tentative listing of compounds would be pentane, heptane, decane, hexadecane, benzene, and toluene. These tests would be conducted with the existing T63 hardware.

The second question concerning the effect of spray cone angle and airflow on getting drops to the igniter could be addressed by taking drop-size measurements with a point-measuring instrument such as a phase-Doppler particle analyzer at the spark gap and comparing with measurements at the fuel nozzle exit. These tests would be performed with atomizers that differed only in cone angle, and would be performed in the existing T63 hardware. The flow of drops from the atomizer to the igniter could be modeled with a computational fluid dynamics code such as FLUENT.

The third question regarding the applicability of the characteristic time model to ignition in combustors using pure airblast atomizers for ignition could be addressed by conducting ignition measurements in a sector of an F100 combustor using a pure airblast atomizer.

The fourth concern about the relative importance of fuel temperature and air temperature could be addressed with tests similar to those reported here but with an independent variation of fuel and air temperatures.

The fifth area of research concerning the temperature history of the ignition kernel is basic to understanding the fundamental droplet evaporation and chemical kinetic processes that take place prior to the ignition event.

The concept of ignition mechanism proposed in Fig. 42 needs to be examined further in a bench-style experiment where more advanced laser diagnostic techniques such as CARs and laser-induced fluorescence could be used to make nonintrusive measurements of temperature and free radical concentration in the ignition kernel.

VII. REFERENCES

1. Moses, C.A., "Studies of Fuel Volatility Effects on Turbine Combustor Performance," Presented at the 1975 Joint Central/Western States Section Spring Meeting of the Combustion Institute, San Antonio, Texas.

2. Gleason, C.C., et al., "Evaluation of Fuel Character Effects on F101 Engine Combustion System," Final Technical Report AFAPL-TR-79-1018, CEEDO-TR-79-07, June 1979.

3. Vogel, R.E. and D.L. Troth, "Fuel Character Effects on Current High Pressure Ratio, Can-type Turbine Combustion Systems," Final Technical Report AFAPL-TR-79-2072, ESL-TR-79-29, April 1980.

4. Oller, T.L., et al., "Fuel Mainburner/Turbine Effects," Final Technical Report AFWAL-TR-81-2100, May 1982.

5. Gleason, C.C. et al., "Evaluation of Fuel Character Effects on J79 Engine Combustion System," Final Technical Report AFAPL-TR-79-2015, CEEDO-TR-79-06, June 1979.

6. Gleason, C.C., et al, "Evaluation of Fuel Character Effects on J79 Smokeless Combustor," Final Technical Report AFWAL-TR-80-2092, ESL-TR-80-46, November 1980.

7. Reider, S.B., Vogel, R.E. and Weaver, W.E., "Effect of Fuel Composition on Navy Aircraft Engine Hot Section Components," Report No. DDAEDR11135 (September 1982).

8. Beal, G.W., "Effect of Fuel Composition on Navy Aircraft Engine Hot Section Components," Report No. PWA/GPD/FR-16456 (August, 1982).

9. Rutter, S.D., "Effect of Fuel Composition on T53L13B Hot Section Components," Report No. D12-6-032-83, (March, 1983).

10. Rutter, S.D., "Effects of Fuel Composition on Navy Aircraft Engine Hot Section Components, Lot II-Component Test," G.E. draft report prepared under Contract No. N00140-79-C-0483.

11. Ball, I., Graham, M., Robinson, K., Davis, N., "T76 Alternative Fuels Final Report," Garrett Turbine Engine Company, Report No. 21-4744, (August, 1983).

12. Ballal, D.R. and Lefebvre, A.H., "A General Model of Spark Ignition for Gaseous and Liquid Fuel-Air Mixtures," 18th Symposium (International) on Combustion, The Combustion Institute, Pittsburgh, pp. 1737-46 (1981).

13. Peters, J.E. and Mellor, A.M., "A Spark Ignition Model for Liquid Fuel Sprays Applied to Gas Turbine Engines," Journal of Energy, 6 ($\underline{4}$), p. 272 (1982).

14. Peters, J.E. and Mellor, A.H., "Characteristic Time Ignition Model Extended to an Annular Gas Turbine Combustor," Journal of Energy, 6 ($\underline{6}$), p. 439 (1982).

15. Peters, J.E. and Mellor, A.H., "An Ignition Model for Quiescent Fuel Sprays," Combustion and Flame, ($\underline{38}$), p. 65 (1980).

16. Derr, W.S. and Mellor, A.H, "Characteristic Times for Lean Blowoff in Turbine Combustors," Presented at the Fall Meeting of the Western States Section/The Combustion Institute (1986).

17. Naegeli, D.W., Moses, C.A., and Mellor, A.H., "Preliminary Correlation of Fuel Effects on Ignitability for Gas Turbine Engines," ASME 83-JPGC-GT-8.

18. Moses, C.A., et al., "An Alternate Test Procedure to Qualify Fuels for Navy Aircraft, Phase II Final Report, Appendix D. Ignition and Altitude Relight," SwRI-5932-3, NAPC-PE-145C (August 1984).

19. Swithenbank, J., Beer, J.M., Taylor, D.S., Abbot, D., and McCreath, G.C., "A Laser Diagnostic Technique for the Measurement of Droplet and Particle Size

Distribution," _Progress in Astronautics and Aeronautics,_ Vol., 53, pp. 421-447 (1977).

20. Godsave, G.A.E., "Studies on the Combustion of Drops in a Fuel Spray - The Burning of Single Drops of Fuel," _Fourth Symposium (International) on Combustion,_ Williams and Wilkins, Baltimore, MD, pp. 813-830 (1953).

21. Ranz, W.E. and Marshall, W.R., Jr., "Evaporation From Drops," Part 1, _Chem. Eng. Prog.,_ 48, p. 141 (1952), Part 2, Vol. 48, p. 173 (1952).

22. Fenn, J.B., "Lean Flammability Limit and Minimum Spark Ignition Energy," _Industrial Engineering Chemistry,_ 43, p. 2865 (1951).

23. Hardin, M.D., "Calculation of Combustion Efficiency and Fuel-Air Ratio From Exhaust Gas Analysis," Technical Data Report RN73-48, Detroit Diesel Allison Division, General Motor Corporation, Indianapolis, IN, p. 27 (July 1973).

24. Dodge, L.G., "Calibration of the Malvern Particle Sizer," _Applied Optics,_ 23, p. 2415 (1984).

25. Dodge, L.G., "Change of Calibration of Diffraction-Based Particle Sizers in Dense Sprays," _Optical Engineering,_ 23, p. 626 (1984).

26. Felton, P.G., Hamidi, A.A., and Aigal, A.K., "Multiple Scattering Effects on Particle Sizing by Laser Diffraction," Report No. 413HIC (August 1984).

27. Allen, T., **Particle Size Measurement,** 3rd Ed. Chapman and Hall, New York, p. 139 (1981).

28. Simmons, H.C. and Harding, C.F., "Some Effects of Using Water as a Test Fluid in Fuel Nozzle Spray Analysis," ASME 80-GT-90 (1980).

29. Kanury, M.A., **Introduction to Combustion Phenomena,** Gordon and Breach Science Publishers, New York, Paris, and London, p. 130 (1975).

30. Gordon, S. and McBride, B.J., "Computer Program for Calculation of Complex Chemical Equilibrium Compositions, Rocket Performance, Incident and Reflected Shocks, and Chapman-Jouguet Detonations," NASA SP-273 (March 1976).

31. Gülder, O.L., "Flame Temperature Estimation of Conventional and Future Jet Fuels," ASME Paper No. 85-GT-31.

32. Rhee, K.T. and Chang, S.L., "Empirical Equations for Adiabatic Flame Temperatures for Some Fuel-Air Combustion Systems," Combustion Science and Technology, 44, 75 (1985).

33. Glassman, I., **Combustion**, Academic Press, Inc., Harcourt Brace Jovanovich Publishers, New York, p. 87 (1987).

NOMENCLATURE

B	=	Transfer Number
β	=	Drop Evaporation Constant
C_{pa}	=	Heat Capacity of Air, kcal/kg
C_{pf}	=	Heat Capacity of Fuel, kcal/kg
d	=	Sauter Mean Diameter (also SMD)
d_q	=	Spark Kernel Diameter, m
E	=	Activation Energy
E_{min}	=	Minimum Ignition Energy, mJ
FN	=	Flow Number
ΔH_{vap}	=	Heat of Vaporization of Fuel, cal/g
k_a	=	Thermal Conductivity of Air, J/m-s-K
ms	=	Millisecond
ν	=	Fuel Viscosity, m^2/s
P	=	Combustor Pressure, kPa
ϕ	=	Equivalence Ratio
Pr	=	Prandtl Number
R	=	Idea Gas Constant
Re	=	Reynolds Number
ρ_a	=	Air Density, kg/m^3
ρ_f	=	Fuel Density, kg/m^3
σ	=	Surface Tension, dynes/cm
s	=	Seconds
T_{10}	=	10 Percent Boil-Off Temperature, K
T_{eb}	=	Droplet Evaporation Time, ms
T_f	=	Fuel Temperature, K
T_{fl}	=	Flame Temperature, K
$T_{\phi=1}$	=	Stoichiometric Flame Temperature, K
T_{hc}	=	Chemical Kinetic Time, ms
T_{in}	=	Combustor Inlet Temperature, K
T_{sl}	=	Turbulent Mixing Time, ms
V_{ref}	=	Reference Velocity, m/s
V_{sg}	=	Gas Velocity at the Spark Gap, m/s
$\dot{w}_f$	=	Mass Flow Rate of Fuel, kg/s

DISTRIBUTION LIST

DEPARTMENT OF DEFENSE

DEFENSE TECHNICAL INFORMATION CTR
CAMERON STATION   12
ALEXANDRIA VA 22314

DEPT OF DEFENSE
OASD/P&L
ATTN: L/EP (MR DYCKMAN)   1
WASHINGTON DC 20301-8000

CDR
DEFENSE FUEL SUPPLY CTR
ATTN: DFSC-Q (MR MARTIN)   1
CAMERON STATION
ALEXANDRIA VA 22304-6160

DOD
ATTN: DUSDRE (RAT) (DR DIX)   1
        ROOM 3-D-1089, PENTAGON
WASHINGTON DC 20301

DEPARTMENT OF THE ARMY

CDR
US ARMY BELVOIR RESEARCH,
    DEVELOPMENT & ENGINEERING CTR
ATTN: STRBE-VF   10
        STRBE-BT   2
FORT BELVOIR VA 22060-5606

HQ, DEPT OF ARMY
ATTN: DALO-TSE   1
        DALO-TSZ-B (MR KOWALCZYK)   1
        DALO-PLA (DR WILTSHIRE)   1
        SARD-TR (MS VANNUCCI)   1
WASHINGTON DC 20310-0561

CDR
US ARMY MATERIEL COMMAND
ATTN: AMCDE-SS   1
        AMCSM-SP   1
        AMCDE-WH   1
5001 EISENHOWER AVE
ALEXANDRIA VA 22333-0001

DIRECTOR
US ARMY MATERIEL SYSTEMS
    ANALYSIS ACTIVITY
ATTN: AMXSY-CM   1
ABERDEEN PROVING GROUND MD
21005-5006

CDR
US ARMY TANK-AUTOMOTIVE COMMAND
ATTN: AMSTA-RG (MR CHECKLICK)   1
        AMSTA-TSL (MR BURG)   1
        AMSTA-MTC (MR GAGLIO)   1
        AMSTA-RGP (MR RAGGIO)   1
        AMSTA-MLF (MR KELLER)   1
        AMSTA-MC   1
        AMSTA-MV   1
        AMSTA-Z (MR FARKUS)   1
WARREN MI 48397-5000

PROJ MGR, MOBILE ELECTRIC POWER
US ARMY TROOP SUPPORT COMMAND
ATTN: AMCPM-MEP-TM
            (COL BRAMLETTE)   1
7500 BACKLICK ROAD
SPRINGFIELD VA 22150

CDR
THEATER ARMY MATERIAL MGMT
    CENTER (200TH)-DPGM
DIRECTORATE FOR PETROL MGMT
ATTN: AEAGD-MMC-PT-Q   1
APO NY 09052

CDR
US ARMY GENERAL MATERIAL &
    PETROLEUM ACTIVITY
ATTN: STRGP-F (MR ASHBROOK)   1
        STRGP-FE, BLDG 85-3
            (MR GARY SMITH)   1
        STRGP-FT (MR ROBERTS)   1
NEW CUMBERLAND PA 17070-5008

CDR
US ARMY LABORATORY COMMAND
ATTN: AMSLC-TP-PB (MR GAUL)   1
        AMSLC-TP-AL   1
ADELPHI MD 20783-1145

CDR
US ARMY RES, DEVEL & STDZN GROUP
    (UK)
ATTN: AMXSN-UK-RA
            (DR REICHENBACH)   1
BOX 65
FPO NEW YORK 09510-1500

CDR
US ARMY FORCES COMMAND
ATTN: FCSJ-SA   1
FORT MCPHERSON GA 30330-6000

CDR
US ARMY RESEARCH OFFICE
ATTN: SLCRO-EG (DR MANN)   1
        SLCRO-CB   1
P O BOX 12211
RSCH TRIANGLE PARK NC 27709-2211

CDR
US ARMY TANK-AUTOMOTIVE CMD
PROGR EXEC OFF CLOSE COMBAT
PM ABRAMS, ATTN: AMCPM-ABMS   1
PM BFVS, ATTN: AMCPM-BFVS   1
PM 113 FOV, ATTN: AMCPM-M113   1
PM M60 FOV, ATTN: AMCPM-M60   1
APEO SYSTEMS, ATTN: AMCPEO-CCV-S   1
PM LAV, ATTN: AMCPM-LA-E   1
WARREN MI 40397-5000

CDR
US ARMY YUMA PROVING GROUND
ATTN: STEYP-MT-TL-M
            (MR DOEBBLER)   1
YUMA AZ 85364-9103

CDR
US ARMY TANK-AUTOMOTIVE CMD
PROGR EXEC OFF COMBAT SUPPORT
PM LIGHT TACTICAL VEHICLES
ATTN: AMCPM-TVL   1
PM MEDIUM TACTICAL VEHICLES
ATTN: AMCPM-TVM   1
PM HEAVY TACTICAL VEHICLES
ATTN: AMCPM-TVH   1
WARREN MI 40397-5000

PROJ MGR, LIGHT ARMORED VEHICLES
ATTN: AMCPM-LA-E   1
WARREN MI 48397

CDR, US ARMY TROOP SUPPORT
    COMMAND
ATTN: AMSTR-ME   1
        AMSTR-S   1
        AMSTR-E (MR CHRISTENSEN)   1
        AMSTR-WL   1
4300 GOODFELLOW BLVD
ST LOUIS MO 63120-1798

CDR
CHEMICAL RD&E CENTER
ATTN: SMCCR-MUS   1
ABERDEEN PROVING GRD MD
21010-5423

PROJ OFF, AMPHIBIOUS AND WATER
    CRAFT
ATTN: AMCPM-AWC-R   1
4300 GOODFELLOW BLVD
ST LOUIS MO 63120-1798

CDR
US ARMY LEA
ATTN: DALO-LEP   1
NEW CUMBERLAND ARMY DEPOT
NEW CUMBERLAND PA 17070

HQ, EUROPEAN COMMAND
ATTN: J4/7-LJPO (LTC WEIMER)   1
VAIHINGEN, GE
APO NY 09128

CDR
US ARMY FOREIGN SCIENCE & TECH
    CENTER
ATTN: AIAST-RA-ST3 (MR BUSI)   1
FEDERAL BLDG
CHARLOTTESVILLE VA 22901

CDR
US ARMY GENERAL MATERIAL &
    PETROLEUM ACTIVITY
ATTN: STRGP-PW   1
BLDG 247, DEFENSE DEPOT TRACY
TRACY CA 95376-5051

CDR
US ARMY ENGINEER SCHOOL
ATTN: ATSE-CD   1
FORT LEONARD WOOD MO 65473-5000

HQ, US ARMY T&E COMMAND
ATTN: AMSTE-TE-T   1
ABERDEEN PROVING GROUND MD
21005-5006

CDR
US ARMY ORDNANCE CENTER &
    SCHOOL
ATTN: ATSL-CD-CS   1
ABERDEEN PROVING GROUND MD
21005-5006

HQ
US ARMY TRAINING & DOCTRINE CMD
ATTN: ATCD-SL   1
FORT MONROE VA 23651-5000

CDR CONSTRUCTION ENG RSCH LAB ATTN: CERL-ES P O BOX 4005 CHAMPAIGN IL 61820	1	CDR US ARMY AVIATION CTR & FT RUCKER ATTN: ATZQ-DI 1 FORT RUCKER AL 36362

CDR
US ARMY TRANSPORTATION SCHOOL
ATTN: ATSP-CD-MS   1
FORT EUSTIS VA 23604-5000

CDR
US ARMY NATICK RES, DEV & ENGR CTR
ATTN: STRNC-U   1
NATICK MA 01760-5020

CDR
US ARMY QUARTERMASTER SCHOOL
ATTN: ATSM-CDM   1
        ATSM-LL FSD   1
FORT LEE VA 23801

PROJECT MANAGER
PETROLEUM & WATER LOGISTICS
ATTN: AMCPM-PWL   1
4300 GOODFELLOW BLVD
ST LOUIS MO 63120-1798

HQ, US ARMY ARMOR CENTER
ATTN: ATSB-CD-ML   1
        ATSB-TSM-T   1
FORT KNOX KY 40121

CDR
US ARMY LOGISTICS CTR
ATTN: ATCL-CD   1
        ATCL-MS   1
FORT LEE VA 23801-6000

CDR
US ARMY FIELD ARTILLERY SCHOOL
ATTN: ATSF-CD   1
FORT SILL OK 73503-5600

CDR
US ARMY INFANTRY SCHOOL
ATTN: ATSH-CD-MS-M   1
        ATSH-TSM-FVS   1
FORT BENNING GA 31905-5400

CDR
US ARMY ARMOR & ENGINEER BOARD
ATTN: ATZK-AE-AR   1
FORT KNOX KY 40121

DEPARTMENT OF THE NAVY

CDR
NAVAL AIR PROPULSION CENTER
ATTN: PE-33 (MR D'ORAZIO)   10
P O BOX 7176
TRENTON NJ 06828-0176

CDR
DAVID TAYLOR RESEARCH CTR
ATTN: CODE 2759 (MR STRUCKO)   1
ANNAPOLIS MD 21402-5067

PROJ MGR, M60 TANK DEVELOPMENT
ATTN: USMC-LNO   1
US ARMY TANK-AUTOMOTIVE
    COMMAND (TACOM)
WARREN MI 48397-5000

DEPARTMENT OF THE NAVY
HQ, US MARINE CORPS
ATTN: LMM/2   1
WASHINGTON DC 20380

CDR
NAVAL AIR SYSTEMS COMMAND
ATTN: CODE 53632F (MR MEARNS)   1
WASHINGTON DC 20361-5360

CDR
NAVAL RESEARCH LABORATORY
ATTN: CODE 6180   1
WASHINGTON DC 20375-5000

CDR
NAVY PETROLEUM OFFICE
ATTN: CODE 43 (MR LONG)   1
CAMERON STATION
ALEXANDRIA VA 22304-6180

OFFICE OF THE CHIEF OF NAVAL
    RESEARCH
ATTN: OCNR-126 (DR ROBERTS)   1
ARLINGTON VA 22217-5000

CG
USMC RDA COMMAND
ATTN: CODE CBAT   1
QUANTICO VA 22134

DEPARTMENT OF THE AIR FORCE

HQ, USAF
ATTN: LEYSF   1
WASHINGTON DC 20330

CDR
US AIR FORCE WRIGHT AERO LAB
ATTN: AFWAL/POSF (MR DELANEY)   1
WRIGHT-PATTERSON AFB OH
45433-6563

HQ AIR FORCE SYSTEMS COMMAND
ATTN: AFSC/DLF (DR DUES)   1
ANDREWS AFB MD 20334

CDR
SAN ANTONIO AIR LOGISTICS CTR
ATTN: SAALC/SFT (MR MAKRIS)   1
            SAALC/MMPRR   1
KELLY AIR FORCE BASE TX 78241

CDR
WARNER ROBINS AIR LOGISTIC CTR
ATTN: WRALC/MMVR-1
            (MR PERAZZOLA)   1
ROBINS AFB GA 31098

OTHER GOVERNMENT AGENCIES

ENVIRONMENTAL PROTECTION AGENCY
AIR POLLUTION CONTROL   1
2565 PLYMOUTH ROAD
ANN ARBOR MI 48105

US DEPARTMENT OF ENERGY   1
MAIL CODE CE-151
FORRESTAL BLDG.
1000 INDEPENDENCE AVE, SW
WASHINGTON DC 20585